The *Verticillium longisporum* phospholipase VlsPLA$_2$ is a virulence factor targets host nuclei and modulates plant immunity

Vahideh Rafiei[#], Heriberto Vélëz[#], Edoardo Piombo, Mukesh Dubey and Georgios Tzelepis[*]

Department of Forest Mycology and Plant Pathology, Swedish University of Agricultural Sciences, Uppsala Biocenter, Box 7026, SE-750 07 Uppsala, Sweden.

[#] Equal contribution

*Correspondence: Georgios.Tzelepis@slu.se

Abstract

Phospholipases A_2 (PLA_2) are lipolytic enzymes, responsible for phospholipids hydrolysis. The role of PLA_2 in various aspects of cell physiology has been shown, but their involvement in host-microbe interactions remains to be elucidated. The present study investigated the biological function of the secreted $VlsPLA_2$ phospholipase in the phytopathogenic fungus *Verticillium longisporum* with emphasis on its role in host-microbe interactions. The *$VlsPLA_2$* was highly induced in *V. longisporum* during interaction with host plant *Brassica napus*, encoding an active phospholipase A_2. $VlsPLA_2$-overexpression *V. longisporum* strain showed an increased virulence on *Arabidopsis* plants, plausibly by inducing virulence factors. Furthermore, $VlsPLA_2$ are transported to the nucleus, by hijacking VAMPA proteins, causing suppression of PTI-induced hypersensitive response, possibly by modulating the expression of genes involved in plant immunity. In summary, $VlsPLA_2$ acts as a virulence factor by hydrolyzing the hosts nuclear envelope phospholipids, an action that induces signaling cascade, suppressing basal plant immunity responses.

Keywords: effector, nucleus, phospholipase, phospholipids, VAMP, *Verticillium*

Introduction

Phospholipids are essential structural components of plasma membranes, being conserved in living organisms, from bacteria to plants and humans. They form a lipid bilayer with a hydrophobic and hydrophilic environment and are abundant in mitochondrial and nuclear envelopes, whereas they are scarce in the thylakoid membranes[1]. Phospholipases are enzymes that hydrolyze phospholipids into phosphatidic acid (PA), diacylglycerol (DAG), free fatty acids (FFAs) and lysophospholipids (LPLs). Based on the site of glycerophospholipid hydrolysis, phospholipases are categorized in phospholipases A_1 (PLA_1) and A_2 (PLA_2); phospholipases C (PLC); phospholipases D (PLD), and are further subdivided in many families and subfamilies[2]. They play important roles in different aspects of cell physiology including signal transduction, cytoskeletal dynamics, and protein secretion[3]. They are also involved in plant defense mechanisms probably as early signaling molecules[4]. Previous studies showed that secreted phospholipases are involved in the regulation of different processes in bacterial and fungal pathogens, but their precise roles in fungal virulence remain unknown[5,6].

Pathogens secrete a plethora of small proteins, termed effectors, in order to avoid plant immunity mechanisms and to establish a successful infection[7]. These proteins can have diverse functions: for example to induce necrosis; to suppress the hypersensitive response (HR); to protect fungal hyphae from host secreting enzymes, such as chitinases; or can be involved in host energy production[8]. Although the sequencing of fungal genomes has helped to identify and understand the diverse roles of fungal effectors, there are still many aspects that remain to be elucidated. From the plant side, the host deploys defense mechanisms to counteract the pathogen's attack and hence, signaling plays a prominent role in this process. As the first layer, the

plasma membrane-localized pattern recognition receptors (PRRs) recognize the microbe associated molecular patterns (MAMPs) (e.g., chitin, flagellin, etc.) and this recognition can lead to a burst of reactive oxidate species (ROS), influx of calcium (Ca^+), the activation of mitogen-activated protein kinases (MAPK) and the induction of defense genes, resulting in pattern triggered immunity (PTI)[9]. When pathogens overcome PTI, then hosts deploy Nod-like receptors (NLRs) able to recognize effectors, leading to effector triggered immunity (ETI)[10]. The outcome of ETI is usually development of HR, although PTI can also result in program cell death[11].

The genus *Verticillium,* which belongs to division Ascomycota in the Plectosphaerellaceae family, includes species causing mainly vascular wilt disease in a plethora of economically important crops[12]. The most important one is the haploid species, *V. dahliae,* which has a broad host range comprising a high number of dicotyledonous plants (e.g., tomato, cotton, olive trees, etc.) [12]. In contrast, the *V. longisporum* species has a narrow host range, infecting mostly plants in Brassicaceae family (e.g., rape seed, cabbage, and broccoli)[13], and is one of the most prominent pathogens in rape seed (*Brassica napus*) cultivation worldwide[13,14,15]. *Verticillium longisporum* is the only non-haploid species in this genus and its genome, characterized as amphidiploid, is the result of hybridization of two species, *V. dahliae* and an unknown lineage[16,17,18]. Progenitors were named A1, D1, D2, and D3, leading to three *V. longisporum* lineage compositions A1/D1, A1/D2 and A1/D3. The origin of A1 and D1 progenitors is unknown, while D2 and D3 derived from two *V. dahliae* lineages[17,18].

In this study, we investigated the role of the secreted phospholipase $VlsPLA_2$ in virulence of *V. longisporum. $VlsPLA_2$* was highly induced during the interaction with *B. napus*. Overexpression of this gene in *V. longisporum* resulted in mutants with

increased fungal virulence, and upregulation of genes coding for variable pathogenicity factors. Furthermore, we confirmed that this protein is an active PLA_2, that seemed to interact with vesicle associated membrane proteins (VAMPs), which are essential compartments of plasma membranes and involved in cellular trafficking [19,20]. This interaction facilitates $VlsPLA_2$ facilitating its transfer to the nuclear envelope and entry to the nucleoplasm, where it altered the expression of genes involved in plant defenses. Lastly, $VlsPLA_2$ was able to suppress the PTI-related HR, induced by the Cf4/Avr4 complex. Taken together, the results from the current study provide a better picture towards understanding the precise roles that these lytic enzymes play in fungal infection biology.

Results

The *$VlsPLA_2$* gene is highly induced during host infection

Verticillium longisporum VL1 isolate contains more than 80 genes encoding putative candidate effector proteins[21]. Since the up-regulation of genes during host infection is a criterion used to classify the encoded protein as an effector[8], we prioritized 13 predicted singletons from the VL1 genome and studied their transcription patterns during infection. Among these genes, only seven showed to be expressed during interaction with the host. The *VL1_T00014035* gene, encoding a putative phospholipase A_2 (denominated as $VlsPLA_2$), was highly upregulated in *V. longisporum* during interaction with *B. napus* roots compared to the mycelium, grown in potato dextrose broth (PDB). (Supplementary Fig. S1). The *$VlsPLA_2$* gene transcription pattern showed the highest induction at six days post infection (Supplementary Fig. S1). Since the role of secreted A_2 phospholipases in fungal virulence are understudied, this gene was selected for further analysis.

VlsPLA$_2$ is a functional phospholipase A$_2$ enzyme

Analysis of *V. longisporum* genome identified two alleles of the *VlsPLA$_2$* gene (*VL1_T00014035* and *VL1_T00011351)*. Conserved domain analysis using translated amino acid sequences of VlsPLA$_2$ identified a conserved phospholipase A$_2$ domain (IPR015141), known to be present in fungal and bacterial phospholipase A$_2$ enzymes[22,23]. Furthermore, sequence analysis of VlsPLA$_2$, derived from fungal and bacterial species, showed a conserved CxRHDFGYxN motif, including the catalytic dyad (HD) (Fig. 1a). Further analysis with multiple prediction tools, showed that VlsPLA$_2$ was a putative cytoplasmic effector, while the presence of a chloroplast transit peptide (cTP) and two nuclear localization signals (NLS; one monopartite and one bipartite), were predicted, indicating a nuclear and chloroplast localization of this effector (Fig. 1a).

To study the gene distribution of *PLA$_2$* among fungal species, more than 60 genomes from species in Basidiomycota, Ascomycota, Mucoromycota and Chytridiomycota divisions were screened. Our analysis showed that genes, putatively encoding secreted PLA$_2$, were identified only in Ascomycota species with diverse lifestyles, and especially in classes Sordariomycetes, Dothideomycetes, Eurotiomycetes and Pezizomycetes, (Supplementary Table S1). A phylogenetic analysis on putative PLA$_2$ homologs derived from different fungal species, showed that these proteins grouped in two major clades, and that VlsPLA$_2$ was clustered together with PLA$_2$ from *V. dahliae, Aspergillus* spp. and entomopathogenic species, such as *Metarhizium* and *Cordyceps* (Fig. 1b). Analysis of the predicted 3D protein structure revealed 54% identity with the PLA$_2$ from the mycorrhizal ascomycete *Tuber borchii* and 48%

similarity with the PLA_2 from the bacterial species *Streptomyces violaceoruber*[22,23] (Fig. 1c).

To investigate the phospholipase activity, $VlsPLA_2$ was heterologously expressed in *E. coli* cells, tagged with 6xHis epitope, and purified through a His-tag purification resin. Enzymatic assays with the purified protein showed that $VlsPLA_2$ was an active phospholipase A_2 that can degrade the PLA_2 selective substrate, similar to the PLA_2 derived from the venom of *Apis mellifera* that was used as a positive control (Fig. 1d). The role of HD catalytic dyad in enzymatic activity of $VlsPLA_2$[24] was investigated by replacing both amino acids with Alanine. Our results showed that the mutated version of $VlsPLA_2$ (i.e., $VlsPLA_2^{\Delta CD}$) was not able to degrade the selective substrate, confirming the importance of this dyad in its enzymatic function (Fig. 1d).

Heterologous expression of $VlsPLA_2$ increases the amount of certain phospholipids in plants

Since phospholipases are the major factor for phospholipid production in cells, we conducted a lipidomic analysis in order to investigate whether $VlsPLA_2$ was able to change the phospholipid profile in the plant. Thus, the WT and mutated version of this protein (i.e., $VlsPLA2^{WT}$ and $VlsPLA_2^{\Delta CD}$, respectively), were heterologously expressed in *Nicotiana benthamiana* plants and the lipid profiles were analysed using high resolution Quadruple-Time-Of-flight (QTOF) mass spectrometry. We focused our analysis mostly on classes of phospholipids (i.e., phosphatidylcholine (PC) and phosphatidylethanolamine (PE)), which are abundant in plant plasma membranes[1]. Our data showed that the relative amounts of monoacyl-glycero-phosphocholines (LPC) 16:0, and diacyl-glycero-phosphocholines (PC) 36:5 and 36:6, were significantly increased in plants expressing the $VlsPLA_2^{WT}$, as compared to the $VlsPLA_2^{\Delta CD}$ or

mock-inoculated ones (Supplementary Fig. S2), indicating that this phospholipase has an impact in the hosts phospholipid profile.

The *VlsPLA$_2$* phospholipase contributes to the *V. longisporum* virulence

To evaluate the potential involvement of VlsPLA$_2$ in *V. longisporum* virulence, the construction of a deletion strain was attempted. Interestingly, all efforts to delete this gene, either in *V. longisporum* or in *V. dahliae*, resulted in mutants carrying both, the deleted locus, and the WT gene (data not shown). Attempts to segregate the mutated nucleus via multiple single spore isolations, continuously failed. Thus instead, mutants overexpressing the *VlsPLA$_2$* gene (constitutively expressed with the *gpdA* promoter from *Aspergillus nidulans*), in *V. longisporum* were generated. The transcription analysis of six single spore isolates, three overexpressing the WT (i.e., *VlsPLA$_2$+^{WT})* and three the enzymatically inactive gene (i.e., *VlsPLA$_2$+$^{\Delta CD}$*), showed a significantly increase of *VlsPLA$_2$* transcription levels in comparison to WT (Supplementary Fig. 3). The Isolates *VlsPLA$_2$+^{WT}* (3) and *VlsPLA$_2$+$^{\Delta CD}$* (1) were chosen for further analysis, since they showed similar expression levels (Supplementary Fig. 3).

Arabidopsis thaliana plants were inoculated with the *V. longisporum* WT or overexpression strains, and plant growth and disease symptoms were monitored 28 dpi. We observed that plants infected with the *VlsPLA$_2$+^{WT}* strain showed more severe symptoms and smaller rosette, as compared to plants infected with the WT and *VlsPLA$_2$+$^{\Delta CD}$* strains. A higher number of dead plants were observed upon infection with the *VlsPLA$_2$+^{WT}* strain, as compared to the *VlsPLA$_2$+$^{\Delta CD}$* one (Fig. 2a, b, c).

Furthermore, the role of this phospholipase in virulence was investigated by generating *A. thaliana* lines overexpressing the *VlsPLA$_2$* gene. Our results showed that the overexpression lines (*35S::VlsPLA$_2$*) displayed higher percentage of dead

plants and smaller rosette, compared to the free GFP infected plants, indicating higher susceptibility to *V. longisporum* infection compared to the plants that expressed only free GFP (Fig. 2d, e, f). These data indicate that $VlsPLA_2$ has an important contribution to the *V. longisporum* virulence.

Since the $VlsPLA_2$ was highly expressed in *V. longisporum* during interaction with *B. napus* (Supplementary Fig. 1), we analyzed the transcriptome of the $VlsPLA_2{+}^{WT}$ strain to investigate the potential transcriptomic changes that the upregulation of this gene could cause in *V. longisporum* mycelia during infection. Our data showed that more than 1300 genes were differentially regulated in the $VlsPLA_2{+}^{WT}$ strain, as compared to the WT (Fig. 3a; Supplementary Table S2). To test whether these transcriptional changes in $VlsPLA_2{+}^{WT}$ strain was associated with its enhanced phospholipase activity, transcriptome of $VlsPLA_2{+}^{\Delta CD}$ strain was also analyzed. In contrast to the $VlsPLA_2{+}^{WT}$ strain, only 104 genes were differentially expressed in the $VlsPLA_2{+}^{\Delta CD}$ strain compared to the WT (Fig. 3a; Supplementary Table S2). Moreover, among these 1300 genes, 158 were up regulated in the $VlsPLA_2{}^{+WT}$ strain as compared to both the $VlsPLA_2{+}^{\Delta CD}$ and WT (Fig. 3a). Among them, we identified several genes that had been validated for their role in *Verticillium* virulence[25,26,27], such as genes encoding zinc finger proteins, cytochrome monooxygenases, efflux-pump proteins, and a Calpain-A like protein (Fig. 3b; Supplementary table S3), indicating that $VlsPLA_2$ could be a co-regulator of pathogenicity factors in *V. longisporum*.

$VlsPLA_2$ suppresses PTI-related hypersensitive response

It is known that pathogens, especially necrotrophs, secrete a plethora of necrosis-inducing effectors[8]. Thus, we investigated whether $VlsPLA_2$ could have the same function by transiently expressing $VlsPLA_2$ in *N. benthamiana* plants and monitoring

the symptoms daily. No necrosis was observed even seven days after Agro-infiltration (data not shown). Moreover, many pathogens rely on an initial biotrophic stage to establish a successful infection by secreting HR suppressing effectors[28]. Hence, the ability of $VlsPLA_2$ to suppress HR was investigated in the Cf4/Avr4 complex. The Cf4 is a Pattern Recognized Receptor (PRR) from tomato plants, recognized by the Avr4 effector produced by fungal pathogen *Cladosporium fulvum*, leading to PTI-related HR [29,30]. Our results showed that in the area where the $VlsPLA_2^{+WT}$ was previously Agro-infiltrated, a significant reduction of HR was observed, as compared to the areas where the mock inoculation and the empty-vector control were infiltrated (Fig. 4a). In contrast, the enzymatically inactive version (i.e., $VlsPLA_2^{\Delta CD}$), was not able to suppress HR (Fig. 4a). The role of $VlsPLA_2$ in suppressing ETI-induced HR caused by *Pseudomonas syringae* pv *tomato* DC3000 was also investigated. This bacterial strain secretes effectors to the host through a Type III secretion system recognized by the *N. benthamiana* R proteins, leading to a strong HR[31]. Our results showed that $VlsPLA_2$ was not able to suppress ETI-related HR, indicating that this effector is involved only to PTI responses (Fig 4b).

It is known that ROS signaling plays a key role in the induction of HR[32]. Thus, to investigate whether $VlsPLA_2$, could suppress the ROS burst, a luminol-based protocol was used on *N. benthamiana* leaves. ROS burst was significantly induced by chitin and production was significantly reduced on leaves which previously had been treated with the $VlsPLA_2^{+WT}$ protein compared to non-treated leaves (Fig 4c). In contrast, no ROS suppression was observed on leaves treated with the enzymatically inactive protein (i.e., $VlsPLA_2^{\Delta CD}$), suggesting that suppression of HR was possibly attributed to the reduction of ROS burst (Fig 4c).

$VlsPLA_2$ is initially localized to the host nuclei

As previously mentioned, the $VlsPLA_2$ protein sequences contains two putative NLS motifs (Fig. 1a). Thus, to confirm the predicted subcellular localization of $VlsPLA_2$, a construct was made tagging $VlsPLA_2$ with GFP at the C-terminus and transiently expressed in *N. benthamiana* leaves, which were monitored using the confocal microscope 48 and 72 hours post infiltration (hpi). Our observations showed that the protein clearly localized to host nuclei at 48hpi, while it was translocated to plant chloroplasts and cell periphery at 72hpi (Fig. 5a). To investigate whether the predicted NLS were functional, a truncated version of $VlsPLA_2$ was constructed, where both NLS were disrupted (i.e., $VlsPLA_2^{\Delta NLS1NLS2}$). Confocal microscopy showed that this truncated version localized to cell periphery, but no nuclear localization was observed (Fig. 5b). Furthermore, we investigated whether both NLS are critical for nuclear localization and for that reason, truncated versions were constructed where either NLS1 or NLS2 were deleted (i.e., $VlsPLA_2^{\Delta NLS1}$ and $VlsPLA_2^{\Delta NLS2}$). Our analysis showed that both NLS mutants were functional, while the bipartite NLS2 seemed to be more critical for nuclear localization (Supplementary Fig. 4). We also studied whether deletion of the signal peptide (SP) could affect $VlsPLA_2$ localization, thus a version lacking this signal was constructed (i.e., $VlsPLA_2^{\Delta SP}$). No changes in nuclear localization were observed between WT and the $VlsPLA_2^{\Delta SP}$ version (Supplementary Fig. 4). We also investigated the localization of the $VlsPLA_2^{\Delta CD}$ version at 48hpi. Interestingly, we observed that $VlsPLA2^{\Delta CD}$ was localized to the chloroplasts and not able to enter the nucleus, although both NLS were intact, indicating that additional factors could also be involved in its nuclear localization (Fig. 5c).

$VlsPLA_2$ binds to the vesicle associated membrane protein A

In order to investigate, whether $VlsPLA_2$ potentially interacts with plant proteins, the $VlsPLA_2$::GFP-CT was transiently expressed in *N. benthamiana*, pull-downed at 48hpi with GFP-trapped beads, and processed for MS/MS spectrometry. In our analysis, a plethora of potential interactions were identified, as compared to free GFP control (Supplementary Table S4). Fifteen potential interacting proteins were selected for further analysis using yeast-two-hybrid (Y2H) assays and focusing mostly on proteins with a predicted nuclear localization, such as transcription factors, histones, and GTP-binding nuclear Ran proteins (Supplementary Table S4). However, according to our analysis none of these selected proteins were able to interact with the $VlsPLA_2$ phospholipase.

Since MS/MS analysis showed that $VlsPLA_2$ potentially interacts also with variable membrane vesicle proteins, their interaction was further investigated with Y2H assays (Supplementary Table S4). Our results showed that the yeast strains co-transformed with $VlsPLA_2$ and NbS00011956g0004 protein, which is putatively a vesicle-associated membrane protein A (VAMPA), denominated as NbVAMPA-1, was able to grow on auxotrophic selection plates (-His, -Ade, -Leu, -Trp), suggesting physical interactions between $VlsPLA_2$ and NbVAMPA-1 (Fig. 6a). Further, disruption of NLS seemed not to have any impact in this interaction (Fig. 6a). However, the co-IP assays showed that NbVAMPA-1 interacted only with the $VlsPLA_2^{\Delta NLS1NLS2}$ version (Fig. 6b). This possibly is attributed to the localization and amount of the $VlsPLA_2^{\Delta NLS1NLS2}$ protein as compared to the WT version of $VlsPLA_2$. Confocal microscopy confirmed that NbVAMPA-1 was localized to the cell periphery, and co-localization with $VlsPLA_2$ in the plant nuclear membrane was also observed (Fig. 6c; Supplementary Fig. 5a).

In addition, we investigated whether the VlsPLA2$^{\Delta CD}$ was able to interact with the NbVAMPA-1 protein and interestingly, our results showed no interaction between them (Fig. 6a). Further, prediction of the VlsPLA2$^{\Delta CD}$ 3D structure, showed that this mutation did not cause any major change in the protein structure, suggesting that the catalytic residue HD was responsible for the interaction with this vesicle protein.

The NbVAMPA-1 protein structure analysis revealed the presence of a motile sperm protein domain (MSP), which is an ER-anchored receptor involved in interorganelle contacts[33], at the N-terminus and a transmembrane domain (TM) at the C-terminus. Furthermore, genome analysis of *N. benthamiana* revealed the presence of ten genes that were homologs to the NbVAMPA-1 one. Alignment of these ten homologs showed the presence of a conserved motif of nine amino acids (DMQCKDKFL) (Supplementary Fig. 5b). Thus, to investigate the role of the different domains (MSP, TM) mutants were generated (i.e., NbVAMPA1$^{\Delta MSP}$ and NbVAMPA1$^{\Delta TM}$ respectively). Our results showed that the MSP-domain-only was not able to interact with VlsPLA$_2$ (NbVAMPA1$^{\Delta TM}$), similar to the truncated NbVAMPA1 where the MSP domain had been deleted (NbVAMPA1$^{\Delta MSP}$), indicating that the intact vesicle protein is required in order to interact with the VlsPLA$_2$ phospholipase (Supplementary Fig. 5c). Moreover, the importance of the DMQCKDKFL conserved motif in interactions with VlsPLA$_2$ was also investigated. Hence, this conserved motif was mutated (NbVAMPA1$^{\Delta CM}$), and protein interactions were evaluated. Our results showed no interaction between VlsPLA$_2$ and the NbVAMPA1$^{\Delta CM}$ version, suggesting that this conserved motif is important for its binding affinity to VlsPLA$_2$ (Supplementary Fig. 5c).

$VlsPLA_2$ modulates expression of transcription factors and genes involved in plant immunity

To investigate whether the presence of $VlsPLA_2$ could cause any modification in the plant's gene-expression patterns, transcriptome of *N. benthamiana* leaves, transiently expressed $VlsPLA_2^{WT}$ or $VlsPLA2^{\Delta CD}$, was analysed 48 and 72hpi. *N. benthamiana* leaves transiently expressed the empty vector was used as a control. At 48hpi, 1846 genes were differentially expressed (DEGs) in leaves where the $VlsPLA_2^{WT}$ gene was expressed, as compared to 144 genes in plants expressing the $VlsPLA_2^{\Delta CD}$ (Fig. 7a, Supplementary Table S5). Among these DEGs, 788 were up-regulated, and 1062 were down-regulated (Fig. 7a, Supplementary Table S5). Interestingly, the number of DEGs significantly reduced to 168 at 72hpi; among them, 127 were induced and 52 were suppressed (Fig. 7a, Supplementary Table S5).

Since $VlsPLA_2$ initially targets the plant nucleus, we investigated the transcription patterns of genes putatively encoding transcription factors. At 48hpi, in plants where the $VlsPLA_2^{WT}$ was expressed, we found 22 DEGs encoding transcription factors, as compared to plants expressing the $VlsPLA_2^{\Delta CD}$ or the empty vector (Fig. 7b, Supplementary Table S5). Among them, three were induced and 19 suppressed (Fig. 7b, Supplementary Table S5). Within the down-regulated ones, we found four genes encoding ethylene-responsive transcription factors, four genes encoding basic helix-loop-helix (bHLH) transcription factors, and five genes encoding myeloblastosis (MYB) transcription factors (Fig. 7b, Supplementary Table S5). Moreover, we studied whether the $VlsPLA_2$ phospholipase could modulate genes involved in plant immunity. At 48hpi, our data showed that six genes encoding putative receptor-like protein kinases (RLKs) and five genes encoding for Avr9/Cf-9 rapidly elicited proteins (ACRE), were highly induced on plants expressing $VlsPLA_2^{WT}$, compared to plants where the $VlsPLA2^{\Delta CD}$

or the empty vector were expressed (Fig. 7c, Supplementary Table S5). On the other hand, *VlsPLA*$_2^{WT}$ expression led to the suppression of 14 genes encoding putatively subtilisin-like proteases and F-box proteins, and three genes encoding aquaporins (Fig. 7c, Supplementary Table S5). In summary, the data from this analysis indicated that VlsPLA$_2$ was a strong modulator of plant immunity responses.

Discussion

In the current study, we investigated the functional role of a fungal secreted PLA$_2$ enzyme, with emphasis on its involvement in infection biology of the phytopathogen *V. longisporum*. Identification of PLA$_2$ genes only in 28 fungal genomes showed patchy distribution of this gene across the fungal kingdom, with no clear correlation to ecological niches or lifestyles. This result is in line with the previous finding, which suggested that *PLA*$_2$ probably derived through horizontal gene transfer from a prokaryotic ancestor to *V. longisporum*[34]. The expression of *VlsPLA*$_2$ was induced in *V. longisporum* during interaction with *B. napus* roots. This is consistent with the previous findings where induction of a gene encoding a secreted *PLA*$_2$ was observed during the establishment of symbiosis in the mycorrhizal species, *Tuber borchii.* It was also activated during autoproteolytic activity and promoted mycorrhiza development with a specific host plant[23,35,36], suggesting that secreted PLA$_2$ could play an important role in different aspects of fungal-host interactions.

Previous studies regarding the role of secreted PLA$_2$ in virulence have been conducted mainly in bacterial-mammalian cell interactions, in which they have been shown to work as toxins inducing proteolysis and hemolysis (e.g., ExoU produced by *Pseudomonas aeruginosa* and SlaA produced by Group A *Streptococcus*), and thereby increasing disease severity[37,38]. It has been proposed that secreted bacterial

390 PLA_2 could degrade the phospholipid components in the host plasma membranes,
391 releasing arachidonic acid (AA) and the subsequent synthesis of eicosanoids, which
392 interferes in signal transduction cascades, altering the transcription of genes and
393 leading to increased inflammatory responses[6]. A similar function could be speculated
394 for the $VlsPLA_2$ phospholipase during interactions with the plant host. Our data from
395 this study showed that that overexpression of *$VlsPLA_2$* in fungal cells resulted in
396 increased *V. longisporum* virulence, and heterologous expression of this
397 phospholipase in *A. thaliana* led to an increased susceptibility against this pathogen.
398 To establish a mechanistic connection between *$VlsPLA_2$* overexpression and
399 increased virulence, transcriptome of both *V. longisporum* mycelia and *N.*
400 *benthamiana* leaves, overexpressing *$VlsPLA_2$*, were analyzed. Induced expression of
401 a diverse range of virulence factor genes, encoding zinc finger proteins, cytochrome
402 monooxygenases, efflux-pump proteins, and a Calpain-A like protein[25,26,27] was
403 observed, indicating that this phospholipase is involved in signal transduction
404 cascades in fungal cells, altering the expression of genes and leading to increased
405 virulence. Similarly, the transcriptome analysis of *N. benthamiana* leaves showed that
406 expression of $VlsPLA_2$ was able to induce RLKs and ACREs, which encode signalling
407 pathways involved in the initial stages of defence responses[39]. We also observed that
408 expression of this phospholipase suppressed many genes encoding MYB and bHLH
409 transcription factors in the plant. These types of transcription factors have been shown
410 to be involved in the regulation of plant defence mechanisms, such as jasmonic acid
411 (JA)-mediated and HR-triggered responses[40,]. In addition, expression of $VlsPLA_2$ led
412 to suppression of a number of genes encoding subtilisin-like proteases and F-box
413 proteins. Their role in the activation of downstream immune responses, including
414 involvement in PTI-related HR, has already been shown[41,42,43] Moreover, these data

were supported by the result that $VlsPLA_2$ was able to suppress PTI-related HR, but not the ETI-induced one, indicating that this phospholipase plays a role only in suppression of basal immune responses. Taken together, these data indicate that $VlsPLA_2$ is a strong modulator of basal plant immune responses.

The nuclear localization of PLA_2 was previously observed in human endothelial cells, and in *Arabidopsis thaliana* plants[44,45]. Especially in *A. thaliana*, PLA_2 suppresses cell death[45], similar to the $VlsPLA_2$ one. It has previously been showed that the nuclear translocation of a cytosolic PLA_2 elicits localized hydrolysis of phospholipids in rat cells[46]. This agrees with our data, showing that $VlsPLA_2$ increased the production of certain phospholipids; thus, we could suggest that the products from this enzymatic function are possibly involved in signal transduction pathways and altering the expression of genes involved in plant immunity. We also found that the $VlsPLA_2$ phospholipase was associated with a plant VAMP-A protein. These are highly conserved proteins present in all eukaryotes and are involved in several physiological functions including membrane trafficking, lipid transport, and unfolded protein response, among others[47]. It has been shown that VAMPs could interact with many different proteins, including proteins involved in plant resistance against fungal pathogens[48,49,50]. Our data showed that NbVAMPA1 promotes the entry of $VlsPLA_2$ to the plant nucleoplasmic reticulum and, presumably, this membrane protein is binding to the active site of $VlsPLA_2$. Similar results have observed in the mammalian cells, where a VAMP-A protein and an oxysterol-binding protein promote the entry of endosomes into the nuclear envelope[51].

In conclusion, the role of a secreted $VlsPA_2$ enzyme in the virulence of the phytopathogenic fungus *V. longisporum* has been investigated. This phospholipase is a regulator of fungal genes, involved in virulence and targets the plant nuclei by

hijacking the VAMP membrane proteins. Once there, $VlsPA_2$ suppresses the expression of genes that play a crucial role in induction of basal immune responses, possibly through the production of phospholipids and their involvement in signal transduction cascades. To the best of our knowledge, this study is the first to examine in detail a fungal secreted PLA_2, by giving important insights about its role in fungal infection biology.

Material and Methods

Fungal strains and growth conditions

In the current study, the *V. longisporum* isolate VL1 (CBS110220) was used. The fungus was kept on potato dextrose agar (PDA, Difco) at 20°C in darkness and sporulation occurred within seven days on this medium.

Nucleic acids manipulation and gene expression analysis

DNA was extracted using the NucleoSpin Plant II kit (Macherey-Nagel GmbH), while RNA was extracted using the Spectrum Plant Total RNA kit (Sigma). RNA was reverse transcribed using the iScript cDNA synthesis kit (Bio-Rad) and the qPCR analysis was done using the SsoFast EvaGreen supermix (Bio-Rad). All PCR reactions were done using Phusion Hot Start II High-Fidelity PCR Master Mix (Thermo Scientific). All PCR products were gel-purified using the GeneJET Gel Extraction Kit (Thermo Scientific). One Shot® TOP10 Chemically Competent *E. coli* (Invitrogen) was used for routine cloning and plasmids were isolated using the GeneJET Plasmid Miniprep Kit (Thermo Scientific). All the kits were used following the manufacturers' protocol.

The transcription profiles of *V. longisporum* genes encoding candidate effector proteins were investigated under conditions previously described[52]. Briefly, *B. napus*

seedlings cultivar ''Hannah'' were inoculated with *V. longisporum* by dipping in 10^6 conidia/ml suspension for 15min. Plants were harvested at 2-, 4-, 6-, 8- and 10-dpi and frozen in liquid nitrogen, while mycelia grown in potato dextrose broth (PDB, Difco) were used as a control. RNA was extracted and treated with DNase I (Thermo Fisher Scientific). For RT-qPCR, one µg of total RNA was reverse transcribed and used for the analysis. Primers sequences are listed in Supplementary Table S6, and gene expression was normalized using the reference gene, glyceraldehyde phosphate dehydrogenase (*GAPDH*)[53]. Relative expression values were calculated from the threshold cycle (Ct) values according to the $2^{-\Delta\Delta CT}$ method[54].

Protein sequence analysis, structure prediction, and phylogeny

The amino acid sequence of $VlsPLA_2$ was retrieved from the *V. longisporum* VL1 genome[21]. Analysis of conserved domains was performed using the SMART protein tools[55]. To investigate whether $VlsPLA_2$ is an apoplastic or a cytoplasmic effector, the ApoplastP prediction tool was used, and its subcellular localization was predicted using the LOCALIZER software[56,57].

Fungal genomes retrieved from the MycoCosm database and searched for putative secreted *PLA_2* genes[58]. For the phylogenetic analysis, homologs to $VlsPLA_2$ were retrieved and the amino acid sequences were aligned with CLUSTAL W and analysis was implemented in MEGA X, using the JTT amino acid substitution model[59]. Statistical support for branches was supported by 1000 bootstraps. Finally, prediction of the $VlsPLA_2$ 3D structure was conducted using the SWISS-MODEL server[60].

Plasmids and vectors generated in the study

Gene fragments for $VlsPLA_2$ and NbVAMPA1 WT and truncated versions, were amplified from *V. longisporum* or *N. benthamiana* cDNA, respectively, or synthesized

and inserted in the pUC19 plasmid by Integrated DNA Technologies (Coralville, IA). They were subcloned into the entry vector pDONOR/Zeo (Invitrogen) using Gateway™ BP Clonase™ enzyme mix (Invitrogen), by following the manufacturer's protocol. The different entry vectors were cloned with the Gateway™ LR Clonase™ enzyme mix (Invitrogen), to the destination vectors, showed in Supplementary Table S7. The expression of genes *in planta,* were driven by the *35S::CaMV* constitutive promoter.

To overexpress VlsPLA2+^{WT} or VlsPLA2+$^{\Delta CD}$ in the fungus, the pRFHUE vector was used, which contains the *gpdA* constitutively expressed promoter. Briefly, the wild type phospholipase gene (VlsPLA$_2^{WT}$) was amplified from *V. longisporum* cDNA, while the VlsPLA$_2^{\Delta CD}$ gene was amplified from the plasmid pUC19-VlsPLA$_2^{\Delta CD}$. The genes and the backbone of the vector were amplified using the primers enlisted in the Supplementary Table S6. The PCR products were gel purified and ligated using the GeneArt™ Seamless Cloning and Assembly Enzyme Mix (Invitrogen), following the manufacturer's protocol.

Heterologous protein expression and enzymatic activity assay

The subcloning, expression, and purification of the active (VlsPLA$_2^{WT}$) and inactive (VlsPLA2$^{\Delta CD}$) protein was done at the Protein Expertise Platform (PEP) at Umeå University. Briefly, Origami2 (DE3) cells were grown in LB media supplemented with 50 µg/mL kanamycin at 37°C with agitation. The culture was incubated until an OD_{600} ~ 0.6–0.7 was achieved. Protein expression was induced by the addition of 0.4 mM isopropyl β-D-1-thiogalactopyranoside (IPTG) and incubated overnight at 20°C. Cells were harvested by centrifugation 4000 x g for 20min. The target protein was purified using His-Tag Purification Resin (Roche) according to the manufacturer instructions.

The His-Trx-tag was cleaved off using Prescission3C protease. Finally, the protein was run on a Superdex200 (Cytiva), 20mM NaP 8.0, 200mM NaCl, 0.5mM b-merchaptethanol. For the phospholipase A_2 enzymatic activity, the EnzChek Phospholipase A_2 activity kit was used (Thermo Fisher), according to manufacturer instructions. In all assays, 10µM of pure active ($VlsPLA_2^{WT}$) and inactive ($VlsPLA2^{\Delta CD}$) protein was used. PLA_2 from *Apis melifera* venom was used as a positive control, and enzymatic activity was monitored at 515 nm using the BMG LABTECH microplate reader.

Lipidomic analysis

For the lipidomic analysis, overnight cultures of *Agrobacterium tumefaciens* (C58C1) harboring either the pGWB602-$VlsPLA_2^{WT}$; pGWB602-$VlsPLA_2^{\Delta CD}$; or the empty vector (i.e., pGWB602) were infiltrated on leaves of 4-week-old *Nicotiana benthamiana* plants (grown under 18h light/6h dark at 23°C). Leaves were harvested at 48hpi and lipids were extracted using the chloroform:methanol (2:1) phase extraction method. The chloroform phase was used for UHPLC-QTOF/MS analysis, using the 1290 Infinity UHPLC (Agilent), coupled to the QTOF 6546 instrument (ODIN) (Agilent), using the parameters previously described for this type of analysis[61]. Data analysis was conducted using the ProFinder 10.0 software (Agilent), by comparing the peaks with the internal database standards for different lipid classes.

Fungal transformation and virulence assays

The vectors pRFHUE-$VlsPLA_2^{WT}$ and pRFHUE-$VlsPLA_2^{\Delta CD}$ were transformed into *V. longisporum* using the *Agrobacterium*-mediated protocol[62]. The selection of transformed fungal strains was accomplished using 50 µg/mL of hygromycin. The

expression levels of the *VlsPLA$_2$* gene in the mutant strains was investigated by RT-qPCR techniques as described above. Single-spore cultures were performed from the five colonies with the highest expression and used for the virulence assays. The growth rate of *V. longisporum* overexpression strains were evaluated on PDA plates. For the virulence assays, the plant species *Arabidopsis thaliana* was used. Seeds were surface sterilized and grown in vitro on half strength Murashige and Skoog medium (½MS; Duchefa Biochemie) for two weeks. Plant infections with *V. longisporum* WT and the overexpression strains (i.e., *VlsPLA$_2^{WT}$* and *VlsPLA$_2^{\Delta CD}$*), as well as mocked-inoculated ones, was conducted as described above. Then, plants were transferred to peat soil and grown in short-day conditions (8 hours light, 16 hours dark) at 23ºC/18ºC for four weeks and watered regularly. The severity of disease was categorized as healthy; mildly infected; severely infected; and dead plants. In addition, the rosette diameter was measured at 28 days post infection.

Construction *of Arabidopsis thaliana* transgenic plants

Agrobacterium tumefaciens strain C58C1 cells carrying the vector pGWB605-VlsPLA$_2^{WT}$, were used to transform *A. thaliana* Col-0 using the floral dip method as and 50 µg/ml of BASTA (glufosinate ammonium) to select for transformants. Expression levels of VlsPLA$_2^{WT}$ in the transgenic lines was confirmed by RT-PCR and Western blot. Two independent homogenous lines in T4 generation were used for the virulence assays, as described above.

Live-cell imaging, hypersensitive response, and ROS burst suppression assays

Overnight cultures of *A. tumefaciens* (C58C1) harboring the vectors, showed in Supplementary Table S7, were infiltrated on leaves of 4-week-old *N. benthamiana*

plants (grown under 18h light/6h dark at 23°C), The subcellular localization of the phospholipase was monitored using a Zeiss LSM 800 confocal microscope at 48 and 72hpi.

For the HR suppression assay, the pGWB602-VlsPLA$_2^{WT}$ and pGWB602-VlsPLA$_2^{\Delta CD}$ vectors were transiently expressed by in *N. benthamiana* plants harboring the Cf-4 receptor protein from tomato plants. The HR was triggered 24hrs after the Agro-infiltration with the *Cladosporium fulvum* Avr4 effector protein at OD_{600} = 0.03. The ability of VlsPLA$_2$ to suppress ETI-triggered HR was investigated on *N. benthamiana* wild type plants upon infection with *Pseudomonas syringae* pv. *tomato* DC3000. Agro-infiltration with empty vector and only induction buffer (mock), were used as controls.

For suppression of chitin-induced oxidative burst of reactive oxygen species (ROS), a luminol-based protocol was used. Briefly, leaf discs from *N. benthamiana* plants, treated with chitin (100 µl/ml), luminol (200µM) (Sigma) and 10 µg/ml horseradish peroxidase (Sigma). The suppression of ROS was analyzed by using 10 µM VlsPLA$_2^{WT}$ and VlsPLA2$^{\Delta CD}$ proteins and measuring the chemiluminescence levels in the BMG LABTECH microplate reader.

MS/MS spectrometry assay

The pGWB605-VlsPLA$_2^{WT}$ vector, was transiently expressed in *N. benthamiana*, while free GFP vector was used as a negative control. Proteins were extracted using an extraction buffer containing 20 mM HEPES pH 6.8, 150 mM NaCl, 1 mM EDTA, 1 mM DTT, 0.5% Tween 20, 1mM PMFS and proteases inhibitor cocktail (Roche) and pull-downed using the GFP-trap agarose magnetic beads (Chromotek). Samples proceeded for LC-ESI-MS/MS analysis at the Clinical Proteomics Mass Spectrometry facility, Karolinska Institute/ Karolinska University Hospital/ Science for Life

Laboratory, Stockholm. On-bead reduction, alkylation, and digestion (trypsin, sequencing grade modified, Pierce) was performed followed by SP3 peptide clean-up of the resulting supernatant. Each sample was separated using a Thermo Scientific Dionex nano LC-system in a 4 hr 5-40 % ACN gradient coupled to Thermo Scientific High Field QExactive. The software Proteome Discoverer vs. 1.4, including Sequest-Percolator for improved identification, was used to search the *N. benthamiana* v044 database for protein identification, limited to a false discovery rate of 1%.

Co-immunoprecipitation and yeast-two-hybrid assays

For the yeast-two-hybrid assays, vectors were transformed into the *Saccharomyces cerevisiae* AH109 strain (Clontech). Transformations with empty vectors were used as negative controls. For co-immunoprecipitation assays, pGWB605-VlsPLA$_2^{WT}$ or pGWB605-VlsPLA$_2^{\Delta NLS1NLS2}$, transiently co-expressed with pGWB614-NbVAMPA1 in *N. benthamiana* and pull-downed as described above for the MS/MS assays. GFP-tagged protein was detected using the B2 anti-GFP HRP-conjugated antibody (Santa Cruz Biotechnology), and HA-tagged proteases were detected using the anti-HA peroxidase-conjugated antibody (Sigma), according to manufacturers' instructions.

RNA sequencing and bioinformatics analysis

For the transcriptomic analysis in *V. longisporum* mycelia, the WT, *VlsPLA2*+^{WT} and *VlsPLA$_2$*+$^{\Delta CD}$ strains were grown in PDB (Difco) for five days at 20°C. For the *in planta* transcriptomic analysis, *N. benthamiana* plants were Agro-infitrated with the pGWB602-VlsPLA$_2^{WT}$ and pGWB602-VlsPLA$_2^{\Delta CD}$ as well as the empty vector (i.e., pGWB602), as described above. The infiltrated leave areas were harvested 48 and 72hpi for RNA extraction. In both cases, total RNA was extracted with the Plant Total

RNA kit (Sigma-Aldrich), and 1000 ng of total RNA was treated with DNase I (Thermo Fisher Scientific), before the generation of RNA strand-specific libraries, using the TruSeq stranded mRNA library preparation kit with polyA selection (Illumina, Inc). Libraries were sequenced using the Illumina NovaSeq 6000 at the SNP&SEQ Technology Platform, Science for Life Laboratory at Uppsala University, Sweden. The experiment was performed in four biological replicates.

The bioinformatics analysis was done as follows. Reads were cleaned and adapters were removed with bbduk v. 38.9[63] with the following parameters: ktrim=r k=23 mink=11 hdist=1 tpe tbo qtrim=r trimq=10). The quality of the trimmed reads was evaluated using the fastqc v.11.9 quality control tool[64]. *Verticillium longisporum* reads were then mapped to *V. longisporum* VL1 genome (accession GCA_001268145.1) using the splice-aware aligner STAR v. 2.7.9a[65] with default parameters. The *N. benthamiana* reads were mapped to the *N. benthamiana* v.5.1 transcriptome (http://sefapps02.qut.edu.au/benWeb/subpages/downloads.php) using the non-splice-aware aligner bowtie2 v. 2.4.2.[66]. The number of reads mapping to each gene was quantified using featureCounts v. 2.0.1[67] considering only sense reads, and differential expression was determined with the DESeq2 R package v. 1.28.1[68] using a minimal threshold of 1 for log2(FC) and 0.05 for FDR adjusted pvalue. Data visualization was performed with R pheatmap module.

For functional annotation, protein sequences were extracted from the genomes and gene coordinates files of *N. benthamiana* and *V. longisporum* using GffRead v. 0.12.2 [69], InterProScan v.5.46.81.0 was used with default parameters to determine additional domains. *V. longisporum* proteins were compared to the PHI-base database v. 09-05-2022[70] using blastp v.2.13.0+ with minimum 80% in both identity and query coverage to determine known factors of virulence.

Conflict of interest

The authors declare no conflict of interest.

Data availability

The transcriptome data of this study (*V. longisporum* and *N. benthamiana* reads) were deposited on ENA database under Bioproject accession number PRJEB55988.

Acknowledgments

We would like to thank Wageningen University for providing us with *N. benthamiana* Cf4 seeds, the Protein Expertise Platform (PEP) for the cloning, expression, and purification of $VlsPLA_2$, and the Swedish Metabolomics Centre (SMC) for the lipidomic analysis at Umeå University. We would also like to thank the Clinical Proteomics Mass Spectrometry facility, at Karolinska Institute, for MS/MS spectrometry, and the SNP&SEQ Platform at SciLife Lab, Uppsala for RNA-seq analyses. We are also grateful to Anna Tornkvist for helping us with the confocal microscopy, and to Jerry Stålberg for the prediction of the $VlsPLA_2$ protein structure and analysis.

References

1. Nakamura, Y. Plant phospholipid diversity: emerging functions in metabolism and protein-lipid Interactions. *Trends in Plant Sci.* **22,** 1027-1040 (2017).
2. Aloulou, A., Ben Ali, Y., Bezzine, S., Gargouri, Y. & Gelb, M.H. Phospholipases: An Overview. *Lipases and Phospholipases: Methods and Protocols* **861,** 63-85 (2012).

3. Hong, Y.Y. et al. Plant phospholipases D and C and their diverse functions in stress responses. *Prog. Lipid Res.* **62,** 55-74 (2016).

4. Zhao, J. Phospholipase D and phosphatidic acid in plant defence response: from protein-protein and lipid-protein interactions to hormone signalling. *J. Exp. Bot.* **66,** 1721-1736 (2015).

5. Ghannoum, M.A. Potential role of phospholipases in virulence and fungal pathogenesis. *Clin. Microbiol. Rev.* **13,** 122-143 (2000).

6. Sitkiewicz, I., Stockbauer, K.E., & Musser, J.M. Secreted bacterial phospholipase A2 enzymes: better living through phospholipolysis. *Trends Microbiol*. **15**, 63-69 (2007).

7. Giraldo, M.C. & Valent, B.. Filamentous plant pathogen effectors in action. *Nat. Rev. Microbiol.* **11,** 800-814 (2013).

8. Lo Presti, L. et al.. Fungal effectors and plant susceptibility. *Ann. Rev. Plant Biol.* **66,** 513-545 (2015).

9. Couto, D. & Zipfel, C. Regulation of pattern recognition receptor signalling in plants. *Nat. Rev. Immunol.* **16,** 537-552 (2016).

10. Boller, T. & Felix, G. A renaissance of elicitors: perception of microbe-associated molecular patterns and danger signals by pattern-recognition receptors. *Annu. Rev. Plant Biol,* **60,** 379-406 (2009).

11. Jones, J.D.G. & Dangl, J.L. The plant immune system. *Nature,* **444,** 323-329 (2006).

12. Pegg, G.F. & Brady, B.L.Verticillium Wilts. Wallingford, Oxfordshire: CABI Publishing (2002).

13. Depotter, J.R. et al. *Verticillium longisporum*, the invisible threat to oilseed rape and other brassicaceous plant hosts. *Mol. Plant Pathol.* **17,** 1004-1016 (2016).

14. Dunker, S., Keunecke, H., Steinbach, P. & von Tiedemann, A. Impact of *Verticillium longisporum* on yield and morphology of winter oilseed rape (*Brassica napus*) in relation to systemic spread in the plant. *J. Phytopathol.* **156,** 698-707 (2008).

15. Tzelepis, G., Bejai, S., Sattar, M.N., Schwelm, A., Ilback, J., Fogelqvist, J. & Dixelius, C. Detection of *Verticillium* species in Swedish soils using real-time PCR. *Arch. Microbiol.* **199,** 1383-1389 (2017).

16. Fahleson, J., Hu, Q. & Dixelius, C. Phylogenetic analysis of *Verticillium* species based on nuclear and mitochondrial sequences. *Arc. Microbiol.* **181,** 435-442 (2004).

17. Inderbitzin, P., Bostock, R.M., Davis, R.M., Usaml, T., Platt, H.W. & Subbarao, K.V. Phylogenetics and taxonomy of the fungal vascular wilt pathogen *Verticillium*, with the descriptions of five new species. *Plos One* **6**, e28341 (2011).

18. Inderbitzin, P., Davis, R.M., Bostock, R.M. & Subbarao, K.V. Identification and differentiation of *Verticillium* species and *V. longisporum* lineages by simplex and multiplex PCR assays. *Plos One* **8**, e65990 (2013).

19. Chen, Y.A. & Scheller, R.H. SNARE-mediated membrane fusion. *Nat. Rev. Mol. Cell Biol*. **2**, 98-106 (2001).

20. Lev, S., Ben Halevy, D., Peretti, D. & Dahan N. The VAP protein family: from cellular functions to motor neuron disease. *Trends Cell. Biol*. **18**, 282-290 (2008).

21. Fogelqvist, J., Tzelepis, G., Bejai, S., Ilback, J., Schwelm, A. & Dixelius, C. Analysis of the hybrid genomes of two field isolates of the soil-borne fungal species *Verticillium longisporum*. *BMC Genom.* **19**, 14 (2018).

22. Matoba, Y., Katsube, Y., & Sugiyama, M. The crystal structure of prokaryotic phospholipase A_2. *J. Biol. Chem*. **277**, 20059-20069 (2002).

23. Soragni, E., Bolchi, A., Balestrini, R., Gambaretto, C., PercudanI, R., Bonfante, P. & Ottonello, S. A nutrient-regulated, dual localization phospholipase A2 in the symbiotic fungus *Tuber borchii*. *EMBO J.* **20,** 5079-5090 (2001).

24. Murakami, M. & Kudo, I. Secretory phospholipase A_2. *Biol. Pharm. Bull.* **27,** 1158-1164 (2004).

25. Tian, L., Yu, J., Wang, Y. & Tian, C. The C2H2 transcription factor VdMsn2 controls hyphal growth, microsclerotia formation, and virulence of *Verticillium dahliae*. *Fungal Biol*. **121**, 1001-1010 (2017).

26. Zhang, T. et al. (2016). Cotton plants export microRNAs to inhibit virulence gene expression in a fungal pathogen. *Nature plants* **2**, 16153 (2016).

27. Santhanam, P. & Thomma, B.P. *Verticillium dahliae* Sge1 differentially regulates expression of candidate effector genes. *Mol. Plant Microbe Interact*. **26**, 249–256 (2013).

28. Stergiopoulos, I. & de Wit, P.J.G.M. Fungal effector proteins. *Annu. Rev. Phytopathol.* **47,** 233-263 (2009).

29. Joosten, M.H.A.J., Vogelsang, R., Cozijnsen, T.J., VErberne, M.C. & de Wit, P.J.G.M. The biotrophic fungus *Cladosporium fulvum* circumvents Cf-4-mediated resistance by producing unstable AVR4 elicitors. *Plant Cell* **9,** 367-379 (1997).

30. van den Burg, H.A., Harrison, S.J., Joosten, M.H.A.J., Vervoort, J. & de Wit, P.J.G.M. *Cladosporium fulvum* Avr4 protects fungal cell walls against hydrolysis by plant chitinases accumulating during infection. *Mol Plant Microbe Interact.* **19:** 1420-1430 (2006).

31. Collmer, A., LIndeberg, M., Petnicki-Ocwieja, T., Schneider, D.J. & Alfano, J.R. Genomic mining type III secretion system effectors in *Pseudomonas syringae* yields new picks for all TTSS prospectors. *Trends Microbiol,* **10:** 462-469 (2002).

32. Zurbriggen, M.D., Carrillo, N. & Hajirezaei, M.R. ROS signaling in the hypersensitive response: when, where and what for?. Plant signal. Behav. **5**: 393–396 (2010).

33. Wendling, C., Spehner, D., Nominé, Y., Giordano, F., Mathelin, C., Drin, G., Tomasetto, C., & Alpy, F. Identification of MOSPD2, a novel scaffold for endoplasmic reticulum membrane contact sites. EMBO reports. **19**: e45453.

34. Shi-Kunne, X., van Kooten, M., Depotter, J.R.L., Thomma, B.P.H.J. & Seidl, M. F. 2019. The genome of the fungal pathogen *Verticillium dahliae* reveals extensive bacterial to fungal gene transfer. Genome Biol. Evol. **11:** 855-868. (2019).

35. Miozzi, L., Balestrini, R., Bolchi, A., Novero, M., Ottonello, S. & Bonfante, P. Phospholipase A(2) up-regulation during mycorrhiza formation in *Tuber borchii.* New Phytol. **167:** 229-238 (2005).

36. Cavazzini, D., Meschi, F., Corsini, R., Bolchi, A., Rossi, G.L., Einsle, O. & Ottonello, S.. Autoproteolytic activation of a symbiosis-regulated truffle phospholipase A(2). J. Biol. Chem. **288:** 1533-1547 (2013).

37. Beres, S.B, et al. Genome sequence of a serotype M3 strain of group A *Streptococcus*: phage-encoded toxins, the high-virulence phenotype, and clone emergence. Proc. Nat.l Acad. Sci. USA. **99**:10078-10083 (2002).

38. Berthelot, P, Attree, I., Plésiat, P., Chabert, J., de Bentzmann, S., Pozzetto, B., Grattard, F; Groupe d'etudes des septicémies à *Pseudomonas aeruginosa*. Genotypic and phenotypic analysis of type III secretion system in a cohort of

Pseudomonas aeruginosa bacteremia isolates: evidence for a possible association between O serotypes and exo genes. J. Infect. Dis. **188**: 512-518 (2003).

39. Rowland, O., Ludwig, A.A., Merrick, C.J., Baillieul, F., Tracy, F.E., Durrant, W. E., Fritz-Laylin, L., Nekrasov, V., Sjölander, K., Yoshioka, H., & Jones, J.D. Functional analysis of Avr9/Cf-9 rapidly elicited genes identifies a protein kinase, ACIK1, that is essential for full Cf-9-dependent disease resistance in tomato. The Plant Cell **17**: 295–310 (2005).

40. Pireyre, M., & Burow, M. Regulation of MYB and bHLH transcription factors: a glance at the protein level. Mol Plant. **8**: 378-388 (2015).

41. van den Burg, H.A., Tsitsigiannis, D.I., Rowland, O., Lo, J., Rallapalli, G., Maclean, D., Takken, F.L., & Jones, J.D. The F-box protein ACRE189/ACIF1 regulates cell death and defense responses activated during pathogen recognition in tobacco and tomato. The Plant Cell. **20**: 697–719 (2008).

42. van der Hoorn, R. Plant proteases: from phenotypes to molecular mechanisms. Annu. Rev. Plant Biol. **59**: 191–223 (2008).

43. Figueiredo, A., Monteiro, F., & Sebastiana, M. Subtilisin-like proteases in plant-pathogen recognition and immune priming: a perspective. Front. Plant Sci. **5:** 739 (2014).

44. Grewal, S., Morrison, E.E., Ponnambalam, S. & Walker, J.H. Nuclear localisation of cytosolic phospholipase A2-alpha in the EA.hy.926 human endothelial cell line is proliferation dependent and modulated by phosphorylation. J. Cell Sci. **115:** 4533-4543 (2002).

45. Froidure, S., Canonne, J., Daniel, X., Jauneau, A., Brière, C., Roby, D.,& Rivas, S. AtsPLA2-alpha nuclear relocalization by the *Arabidopsis* transcription factor

AtMYB30 leads to repression of the plant defense response. Proc. Natl. Acad. Sci. USA. **107**:15281-15286 (2010).

46. Peters-Golden, M., Song, K., Marshall, T. & Brock, T. 1996. Translocation of cytosolic phospholipase A_2 to the nuclear envelope elicits topographically localized phospholipid hydrolysis. Biochem. J. **318**: 797-803 (1996).

47. Lev, S., Ben Halevy, D., Peretti, D., & Dahan, N. The VAP protein family: from cellular functions to motor neuron disease. Trends Cell. Biol. **18**: 282-290. (2008).

48. Petersen, N.H.T., Joensen, J., McKinney, L.V., Brodersen, P., Petersen, M., Hofius, D., Mundy, J. Identification of proteins interacting with *Arabidopsis* ACD11. Plant Physiol. **166**:661-666 (2009).

49. Saravanan, R.S., Slabaugh, E., Singh, V.R., Lapidus, L.J., Haas, T., Brandizzi, F. The targeting of the oxysterol-binding protein ORP3a to the endoplasmic reticulum relies on the plant VAP33 homolog PVA12. Plant J. **58:**817-830 (2009).

50. Kim, H., O'Connell, R., Maekawa-Yoshikawa, M., Uemura, T., Neumann, U., Schulze-Lefert, P. The powdery mildew resistance protein RPW8.2 is carried on VAMP721/722 vesicles to the extrahaustorial membrane of haustorial complexes. Plant J. **79:** 835-847 (2014).

51. Santos, M.F., Rappa, G., Karbanová, J, Kurth, T., Corbeil, D., Lorico, A. VAMP-associated protein-A and oxysterol-binding protein-related protein 3 promote the entry of late endosomes into the nucleoplasmic reticulum. J. Biol. Chem. **293**: 13834-13848 (2018).

52. Rafiei, V., Najafi, Y., Vélëz, H., & Tzelepis, G. Investigating the role of a putative

endolysin-like candidate effector protein in *Verticillium longisporum* virulence, Biochem. Biophys. Res. Commun. **629**: 6-11 (2022).

53. Rafiei, V., Ruffino, A., Persson-Hoden, K., Tornkvist, A., Mozuraitis, R., Dubey, M. & Tzelepis, G. A *Verticillium longisporum* pleiotropic drug transporter determines tolerance to the plant host beta-pinene monoterpene. Mol. Plant Pathol. **23:** 291-303 (2022)**.**

54. Livak, K.J. & Schmittgen, T.D. (2001). Analysis of relative gene expression data using real-time quantitative PCR and the 2(T)(-Delta Delta C) method. Methods*.* **25:** 402-408 (2001).

55. Letunic, I., Doerks, T. & Bork, P. (2009). SMART 6: recent updates and new developments. *Nucleic Acids Res,* **37:** D229-D232.

56. Sperschneider, J., Dodds, P.N., Singh, K.B., & Taylor, J.M. ApoplastP: prediction of effectors and plant proteins in the apoplast using machine learning. New phytol. **217**: 1764–1778 (2018).

57. Sperschneider, J., Catanzariti, A.M., DeBoer, K., Petre, B., Gardiner, D. M., Singh, K. B., Dodds, P.N., & Taylor, J.M. LOCALIZER: subcellular localization prediction of both plant and effector proteins in the plant cell. Sci Rep. **7**: 44598 (2017).

58. Grigoriev, IV et al. “MycoCosm portal: gearing up for 1000 fungal genomes.” Nucleic Acids Res. **42**: D699-704 (2014).

59. Kumar, S., Stecher, G., Li, M., Knyaz, C. & Tamura, K. MEGA X: Molecular evolutionary genetics analysis across computing platforms. Molecul. Biol. Evol. **35:** 1547-1549 (2018).

60. Waterhouse, A., Bertoni, M., Bienert, S., Studer, G., Tauriello, G., Gumienny, R., Heer, F.T., de Beer, T.A.P., Rempfer, C., Bordoli, L., Lepore, R., Schwede,

T. SWISS-MODEL: homology modelling of protein structures and complexes. Nucleic Acids Res. **46**: W296-W303 (2018).

61. Nygren, H., Seppänen-Laakso, T., Castillo, S., Hyötyläinen, T., & Orešič, M. (2011). Liquid chromatography-mass spectrometry (LC-MS)-based lipidomics for studies of body fluids and tissues. Methods Mol. Biol. **708**: 247–257.

62. Utermark, J., & Karlovsky, P. Genetic transformation of filamentous fungi by *Agrobacterium tumefaciens*. Protocol Exchange. http://www.nature.com/protocolexchange/protocols/427, (2008).

63. Bushnell, B. BBTools: A suite of fast, multithreaded bioinformatics tools designed for analysis of DNA and RNA sequence dData. Jt. Genome Inst. Berkeley, CA, USA (2018).

64. Andrews, S. FastQC: a quality control tool for high throughput sequence data. Available at: https://www.bioinformatics.babraham.ac.uk/projects/fastqc/ (2010).

65. Dobin, A., et al. 2013. STAR: Ultrafast universal RNA-seq aligner. Bioinformatics. **29**:15–21 (2013).

66. Langmead, B., & Salzberg, S. L. Fast gapped-read alignment with Bowtie 2. Nat. Methods. **9**: 357–359 (2012).

67. Liao, Y., Smyth, G.K., & Shi, W. FeatureCounts: an efficient general purpose program for assigning sequence reads to genomic features. Bioinformatics. **30**: 923–930 (2014).

68. Love, M.I., Anders, S., & Huber, W. Differential analysis of count data - the DESeq2 package. Genome Biol. **15**:10–1186 (2014).

69. Pertea, G., & Pertea, M. GFF utilities: GffRead and GffCompare. F1000 Research. 9 (2020).

70. Urban, M., et al. PHI-base: A new interface and further additions for the multi-species pathogen-host interactions database. Nucleic Acids Res. **45**:604–610 (2017).

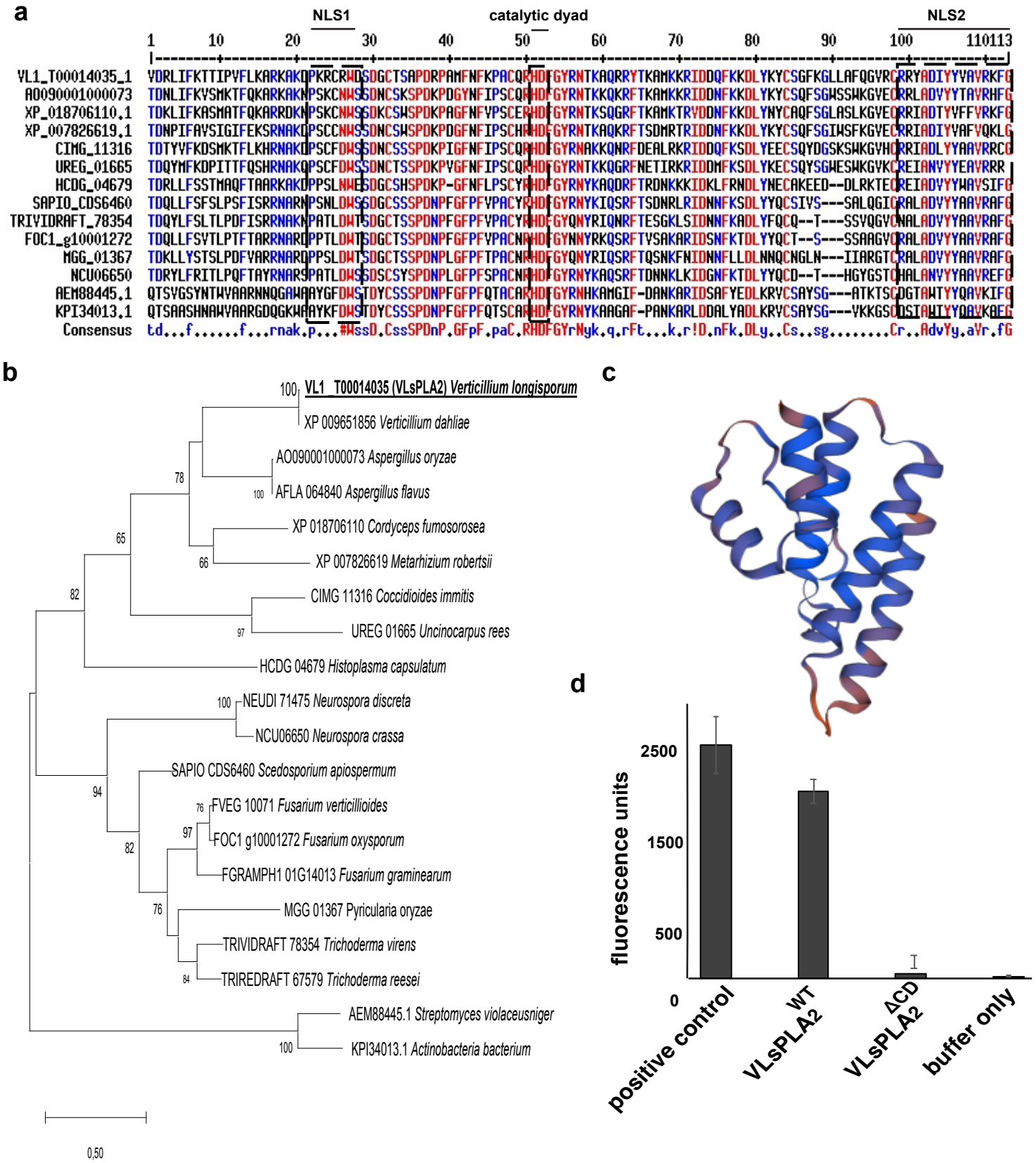

Fig. 1. Analysis of the VlsPLA$_2$ protein. **a.** Alignment of the amino acid sequences of VlsPLA$_2$ and phospholipases derived from different bacterial and fungal species using the Clustal Omega software. Identical amino acids are marked with red color. Different motifs showed in red dashed boxes. The catalytic dyad HD and the two NLS are marked with dashed boxes. **b.** Phylogenetic analysis of the VlsPLA$_2$ protein and phospholipases from different fungal species. Analysis was conducted using the neighbour-joining method with the JTT amino acid substitution model based on amino acid sequences and 1000 bootstraps. Number at nodes indicate the bootstrap values. Bar indicates the number of amino acid substitution. Predicted amino acidic sequences were aligned using the CLUSTAL W algorithm and phylogeny was constructed in the MEGA X software. **c.** Predicted 3D structure of VlsPLA$_2$. The protein model was predicted using the SWISS-MODEL software. **d.** Phospholipase A$_2$ activity assay using 10μM purified VlsPLA$_2^{WT}$ and VlsPLA2$^{\Delta CD}$ proteins. PLA$_2$ from bee venom and buffer-only were used as a positive and negative controls respectively. Error bars represent SE based on eight technical replicates.

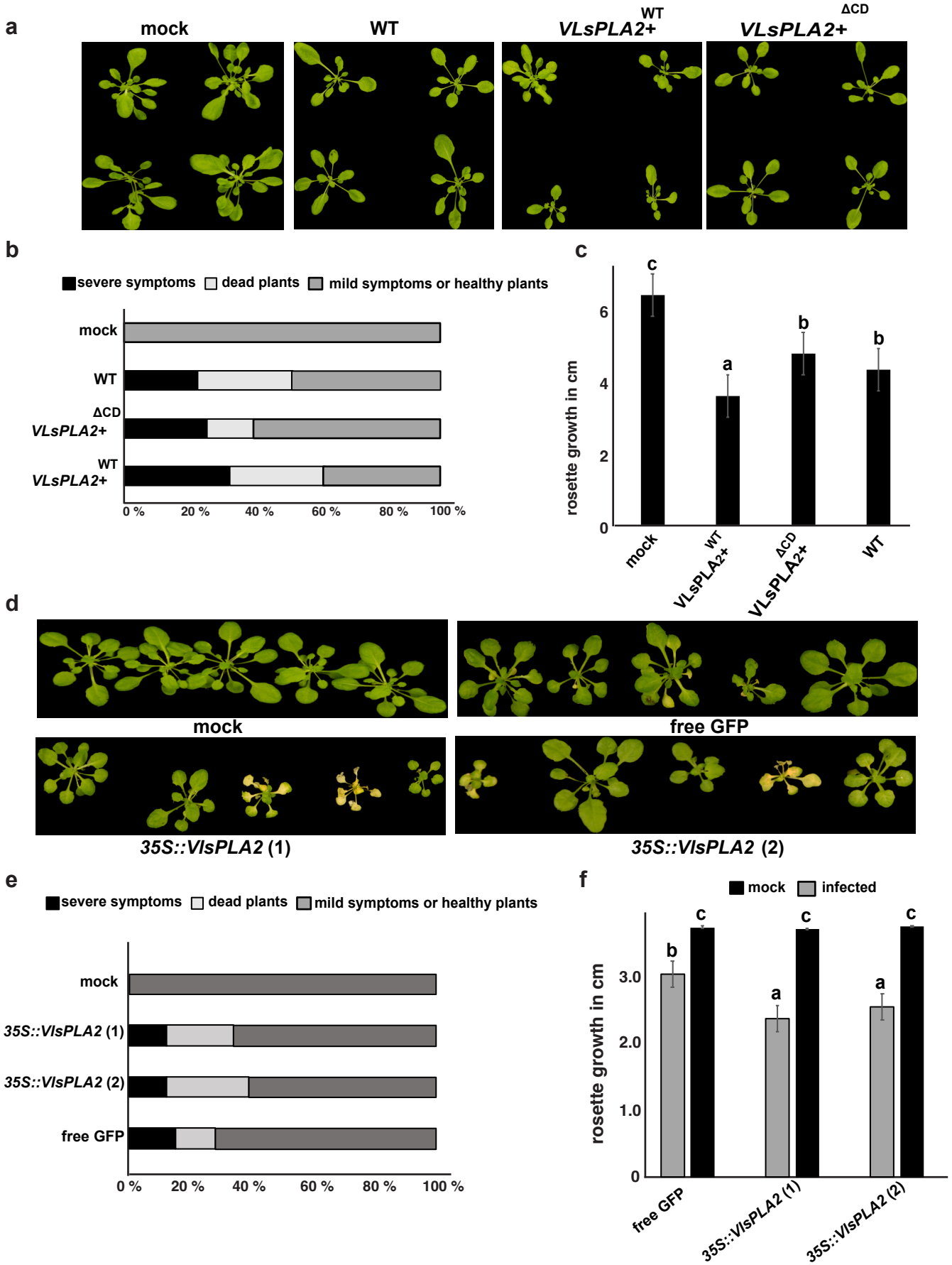

Fig. 2. The VlsPLA$_2$ phospholipase contributes to *V. longisporum* virulence. a. *A. thaliana* plants infected with *V. longisporum* VlsPLA$_2$+^{WT}, VlsPLA$_2$+$^{\Delta CD}$, or the wild type (WT) strains. The experiment was performed in 36 plants. Photographs of representative plants were taken 28 days post inoculation (dpi). Mock-inoculated plants were used as control. **b.** percentage of dead, mild-infected and healthy *A. thaliana* plants 28 dpi with *V. longisporum* VlsPLA$_2$+^{WT}, VlsPLA$_2$+$^{\Delta CD}$ or WT strains. **c.** Rosette growth in cm of *A. thaliana* plants infected with *V. longisporum* VlsPLA$_2$+^{WT}, VlsPLA$_2$+$^{\Delta CD}$, or WT strains 28 dpi. Different letters (a, b ,c) showed statistically significant differences according to Student's T test ($p<0.05$). Error bars represents SE based on at least 36 plants. **d.** Representative *A. thaliana* plants, expressing the VlsPLA$_2$ phospholipase (*35S::VlsPLA$_2$*), 28 days post infection with *V. longisporum*. Mock-inoculated and plants expressing free GFP were used as controls. **e.** Percentage of dead, mild-infected and healthy *35S::VlsPLA$_2$*, free GFP-expressed and mock-inoculated *A. thaliana* plants, 28 dpi with *V. longisporum.* **f.** Rosette growth in cm, of *35S::VlsPLA$_2$*, free GFP-expressed and mock-inoculated *A. thaliana* plants, 28 dpi with *V. longisporum.* Different letters (a, b, c) showed statistically significant differences according to Student's T test ($p<0.05$). Error bars represents SE based on at least 50 plants. Images background has been removed using the Affinity Designer software, without any modification in plants.

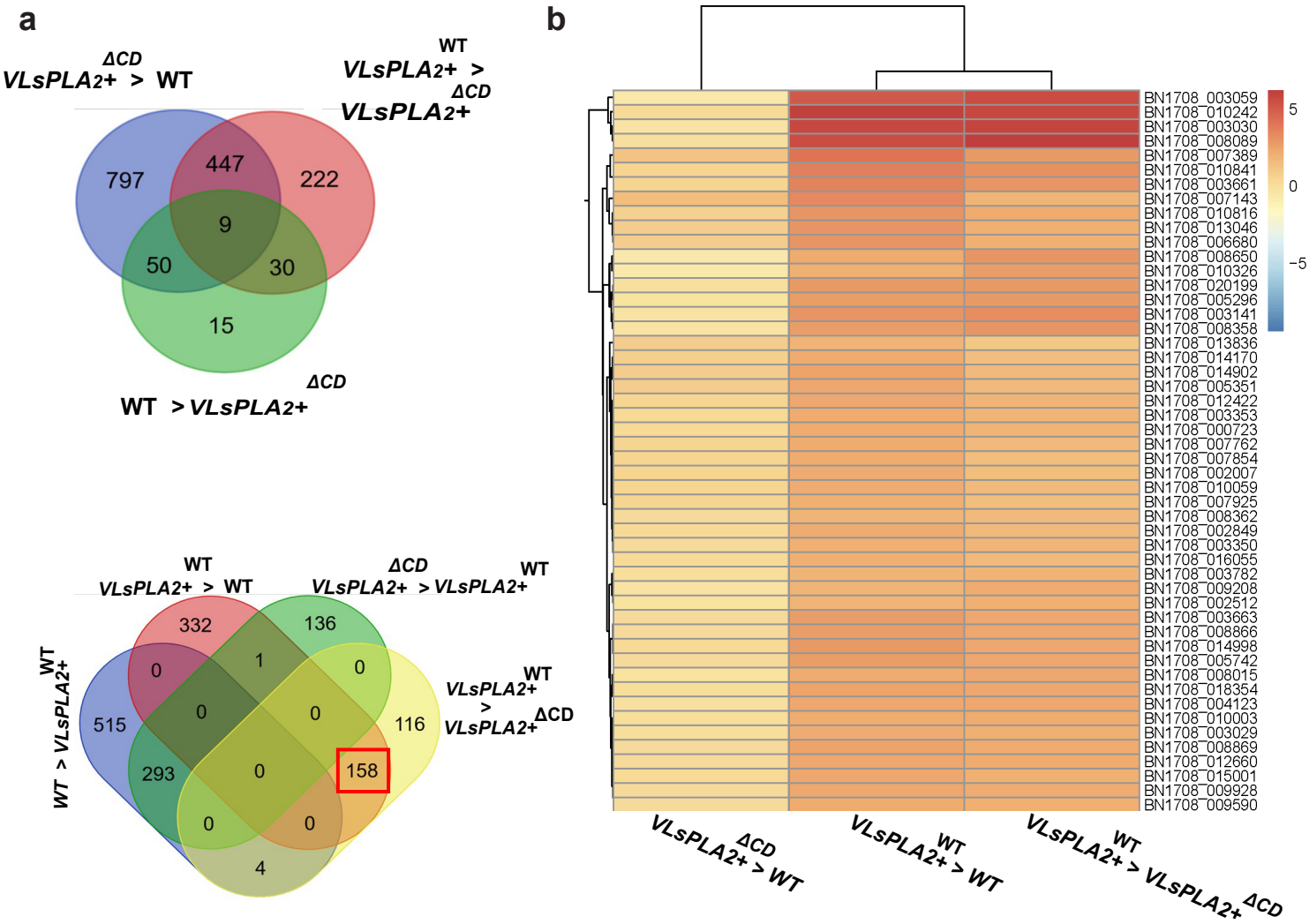

Fig. 3. Overexpression of *VlsPLA$_2$* causes severe transcriptomic changes in *V. longisporum* mycelia a. Venn diagrams show the number of differentially expressed genes in *V. longisporum* mycelia derived from the WT, and the strains overexpressing either the functionally active (VlsPLA$_2$+^{WT}) or the inactive (VlsPLA$_2$+$^{\Delta CD}$) VlsPLA$_2$ phospholipase. The sign ">" show the number of up-regulated genes in each studied comparison. The number of genes of interest are highlighted in a red box. **b.** Heatmap depicts the log2(FC) of the top 50 up-regulated genes in the *V. longisporum* VlsPLA$_2$+^{WT} strain as compared to VlsPLA$_2$+$^{\Delta CD}$ and WT. Adjusted p-value < 0.05, absolute log2 fold change > 2 for up-regulated genes. Analysis was conducted in four biological replicates.

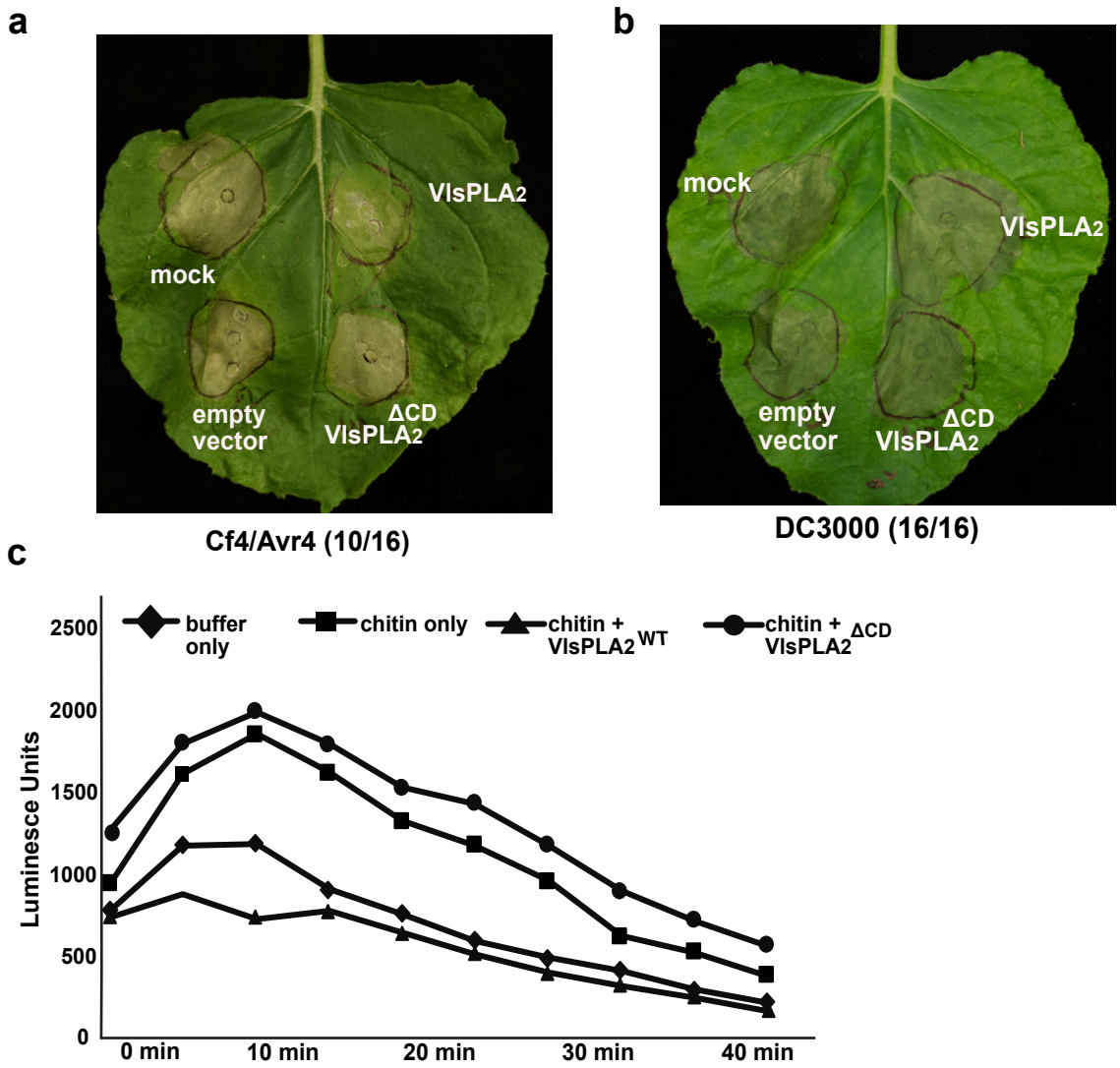

Fig. 4. VlsPLA$_2$ phospholipase negatively regulates PTI-related hypersensitive responses (HR). a. HR suppression assay by VlsPLA$_2^{WT}$ and VlsPLA$_2^{\Delta CD}$ on *N. benthamiana,* expressing the Cf-4 receptor. HR challenged 24 hours post infiltration with the Avr4 effector. **b** HR suppression assay by VlsPLA$_2^{WT}$ and VlsPLA$_2^{\Delta CD}$ on *N. benthamiana.* HR was induced by *P. syringae* pv *tomato* DC3000 24 hours post infiltration. Inoculation with the empty pGWB602 vector and mock inoculation with the induction buffer were used as controls. Images taken 3 days post inoculation. In total eight plants and two leaves per plant were used. **b.** Chitin-induced oxidative (ROS) burst assay in *N. benthamiana* leaves. Production of ROS was determined using luminol-dependent chemiluminescence. Leaf discs were treated with chitin, 10 μM VlsPLA$_2^{WT}$ or VlsPLA$_2^{\Delta CD}$ purified protein, while only buffer was used as a negative control. In total eight biological replicates were used

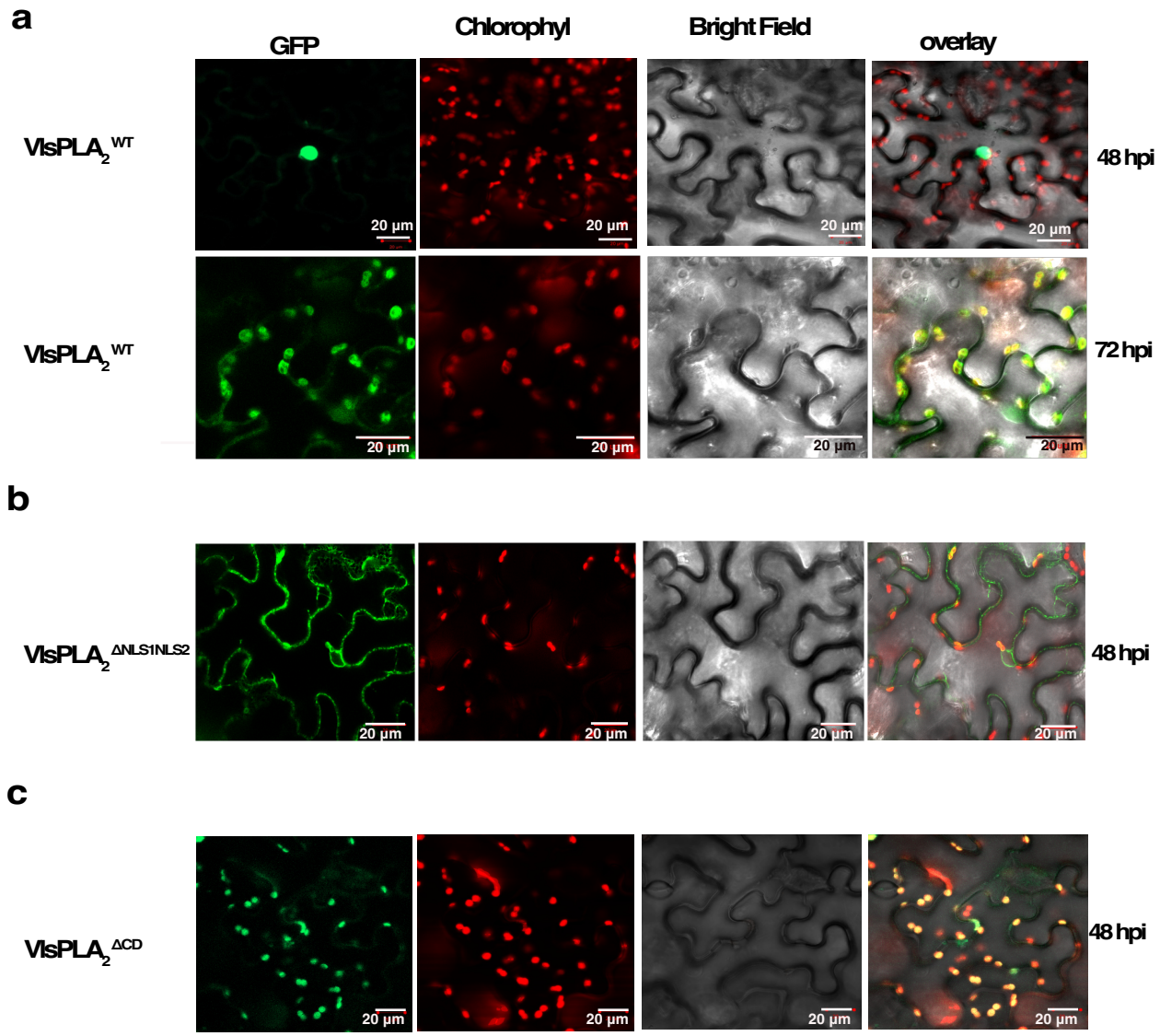

Fig. 5. The VlsPLA$_2$ phospholipase is initially localized to the host nuclei. Live-cell imaging of **a.** VlsPLA$_2^{WT}$, **b.** VlsPLA2$^{\Delta NLS1NLS2}$ and **c.** VlsPLA$_2^{\Delta CD}$ versions, tagged with GFP at the C-terminus in transiently expressed *N. benthamiana* leaves. The localization was monitored with a laser-scanning confocal microscope with a sequential scanning mode 48 and 72 hours post infiltration. The GFP and the chlorophyll were excited at 488 nm. GFP (green) and chlorophyll (red) fluorescent signals were collected at 505– 525 and 680–700 nm, respectively.

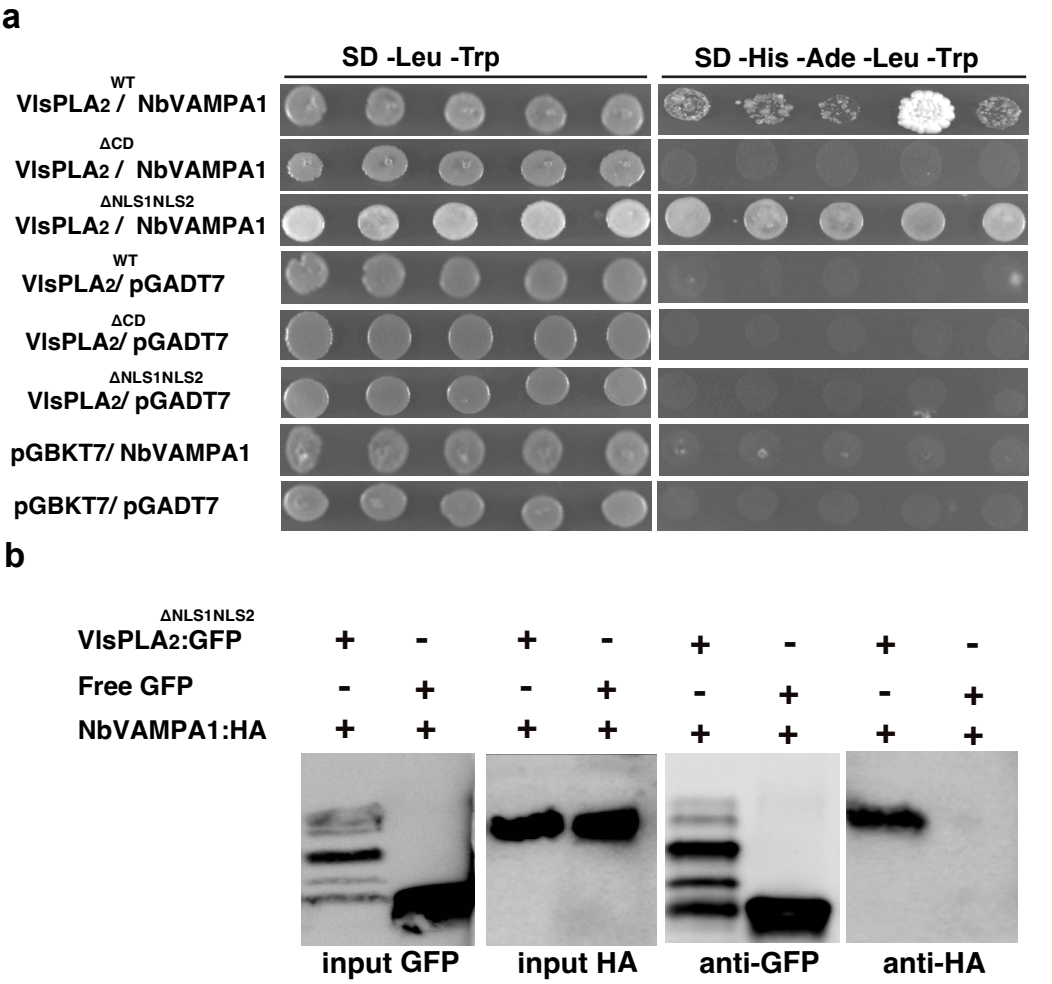

Fig. 6. The VlsPLA$_2$ phospholipase interacts with the plant vesicle protein NbVAMPA1. a. Pairwise yeast-two-hybrid assays between VlsPLA$_2^{WT}$, VlsPLA$_2^{\Delta CD}$ or VlsPLA2$^{\Delta NLS1NLS2}$ (used as a bait in pGBKT7 vector), and NbVAMPA1 protein (used as a prey in pGADT7 vector). Growth of yeast cells on SD-4 (-His, -Ade, -Leu, -Trp) selective media represents protein–protein interaction and growth on SD-2 (-Leu, -Trp) media confirms yeast transformation. Yeast transformed with the empty vectors were used as negative controls. **b**. Co-immunoprecipitation assay (co-IP) assay between the GFP-tagged VlsPLA$_2^{\Delta NLS1NLS2}$ and HA-tagged NbVAMPA1, transiently co-expressed in *N. benthamiana* leaves and pull downed using the GFP-trap agarose magnetic beads. **c**. Live-cell imaging of VlsPLA$_2^{WT}$ tagged with GFP at the C-terminus, and NbVAMPA1 tagged with tagRFP at the N-terminus, in Agro-infiltrated *N. benthamiana* leaves. The localization was monitored with a laser-scanning confocal microscope with a sequential scanning mode 48 hrs post infiltration. The GFP and the chlorophyll were excited at 488 nm. GFP (green) and chlorophyll (red) fluorescent signals were collected at 505– 525 and 680–700 nm, respectively. The tagRFP was excited at 558 nm and collected at 545-620 nm.

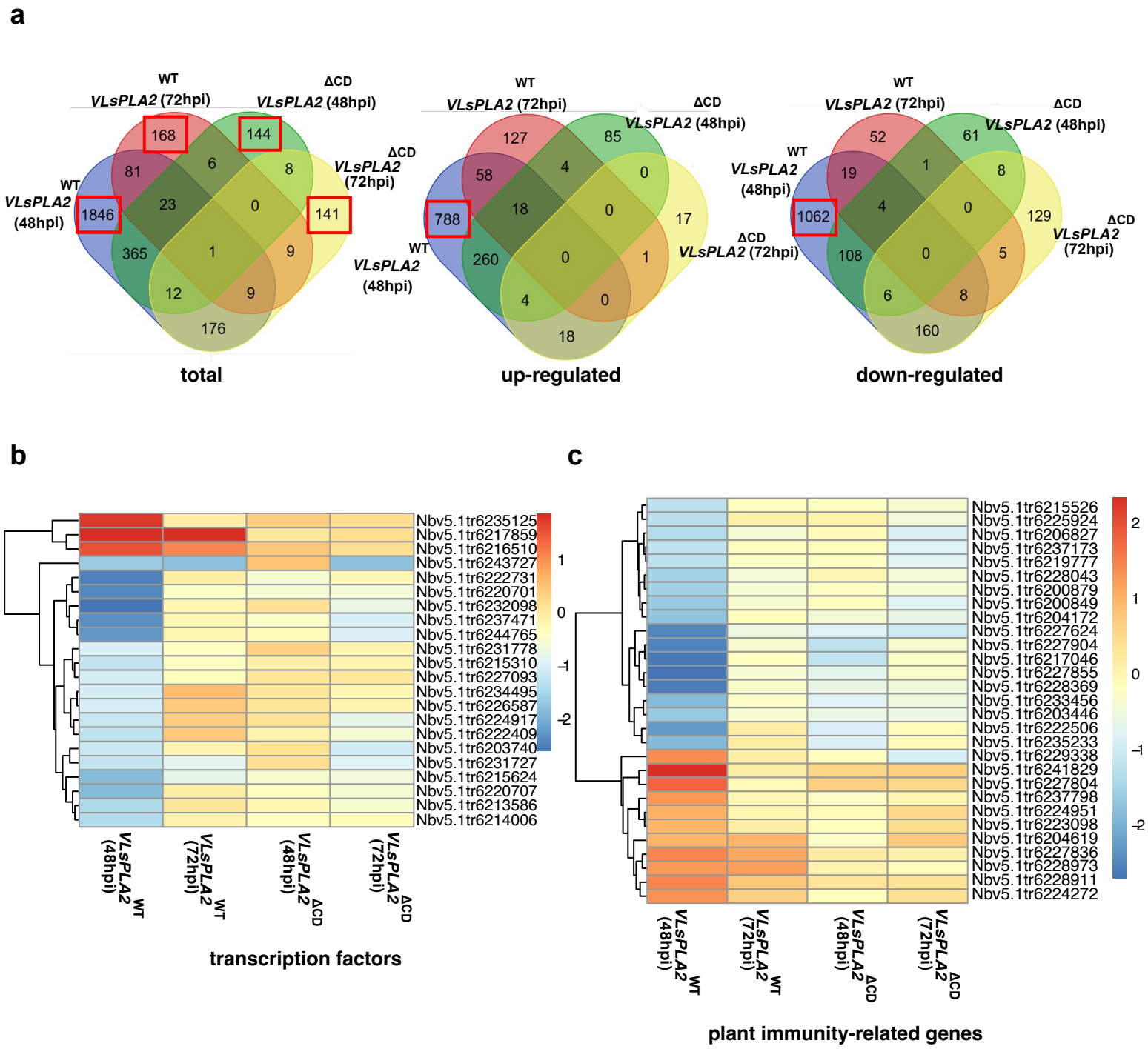

Fig. 7. The *VlsPLA*$_2$ phospholipase modulates plant immunity responses. a. Venn diagrams show the number of differentially expressed genes in *N. benthamiana* plants transiently expressing either the functionally active (VlsPLA$_2^{WT}$) or the inactive (VlsPLA$_2^{\Delta CD}$) VlsPLA$_2$ phospholipase, 48 and 72 hours post infiltration. The number of genes of interest are highlighted in a red box. **b.** Heatmap depicts the log2(FC) of differentially regulated genes putatively encoding transcription factors in *N. benthamiana* plants transiently expressing either VlsPLA$_2^{WT}$ or the VlsPLA$_2^{\Delta CD}$ 48 and 72 hours post infiltration. **c.** Heatmap depicts the log2(FC) of differentially regulated genes putatively encoding plant immunity-related proteins in *N. benthamiana* transiently expressing either VlsPLA$_2^{WT}$ or VlsPLA2$^{\Delta CD}$, 48 and 72 hours post infiltration. In all cases the transcriptome of plants inoculated with the empty vector used as a control. (adjusted p-value < 0.05, log2 fold change > 1 for up-regulated genes and < -1 for the downregulated ones). Analysis was conducted in four biological replicates.

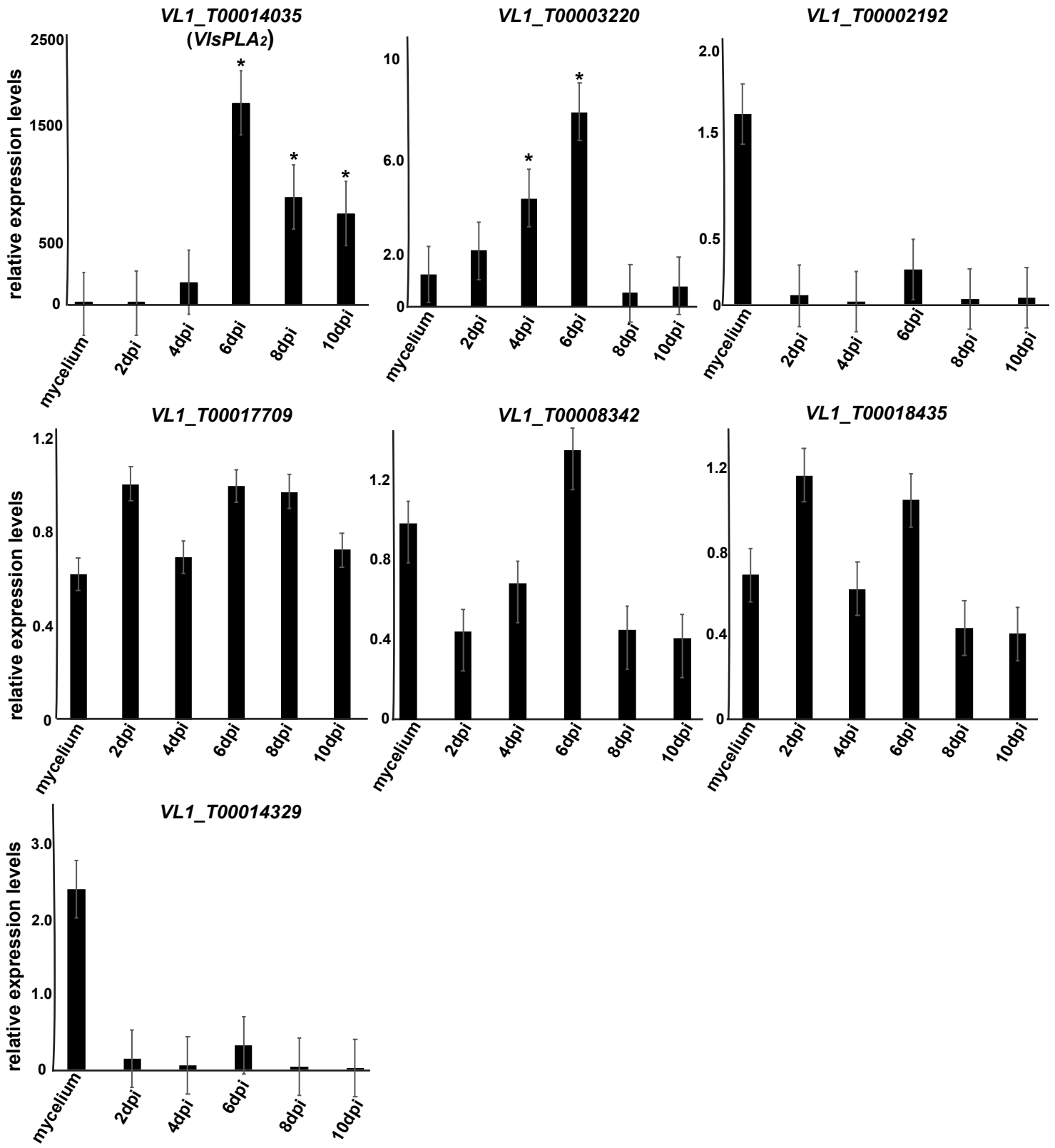

Supplementary Fig. 1. Transcription profiles of *V. longisporum* genes encoding candidate effector proteins upon infection of *Brassica napus.* Gene expression analysis was conducted according to $2^{-\Delta\Delta CT}$ method. Data were normalized using the expression levels of the reference gene, glyceraldehyde phosphate dehydrogenase (*GAPDH*). Error bars represent SE based on at least three biological replicates. Asterisks indicate statistically significant differences according to Students T' test (p value < 0.05).

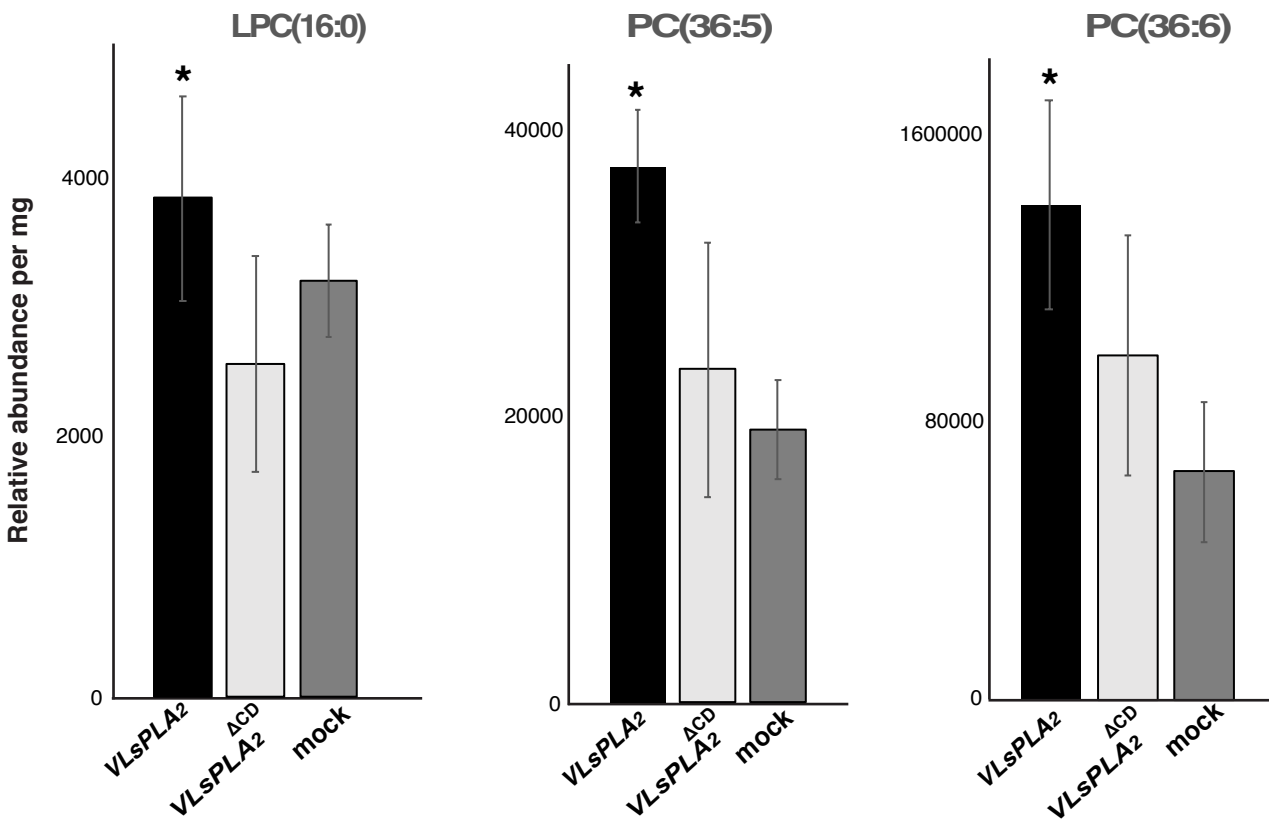

Supplementary Fig. S2. Phospholipid profiles on *N. benthamiana* transiently expressed either $VlsPLA_2^{WT}$ or $VlsPLA_2^{\Delta CD}$. Mocked-inoculated plants were used as control. Data depicted as a relative abundance of phospholipids per mg of dry plant tissue. Asterisks (*) indicate statistically significant differences according to the Student's T test ($p < 0.05$). Bars represent the standard error (SE) based on five biological replicates.

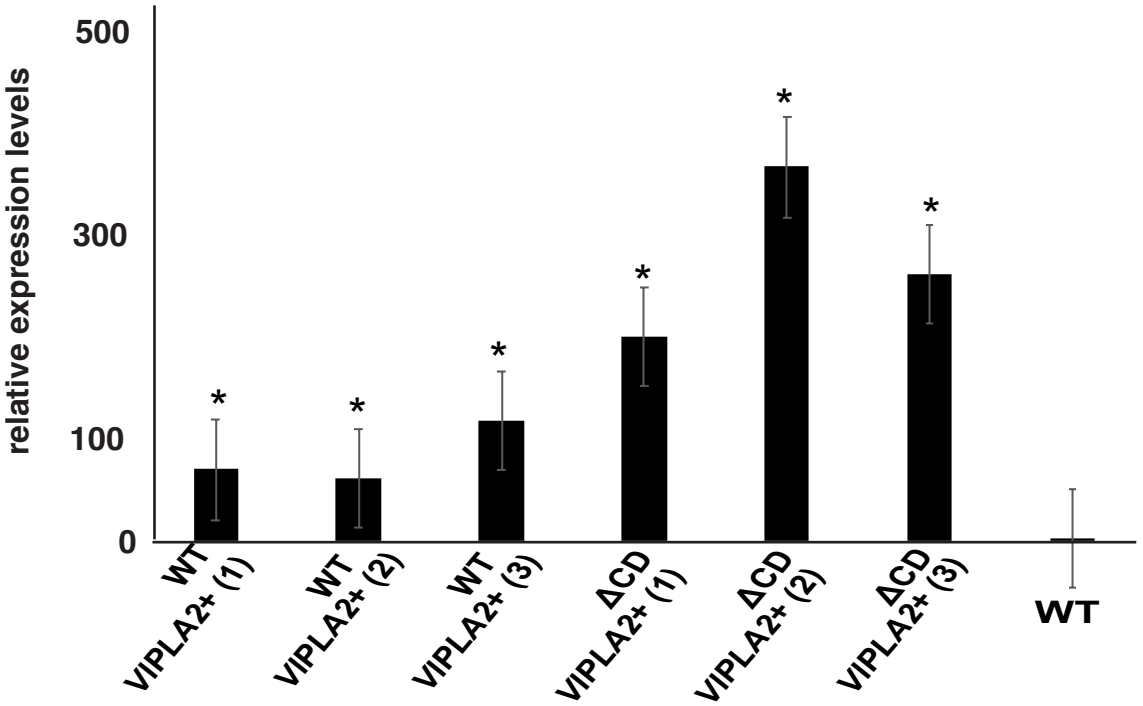

Supplementary Fig. S3. Transcription analysis on *Verticillium longisporum* strains overexpressing either the functional active ($VlsPLA_2$+^{WT}) or the inactive ($VlsPLA_2$ + $^{\Delta CD}$) $VlsPLA_2$ phospholipase. Gene expression analysis was conducted according to $2^{-\Delta\Delta CT}$ method. Data were normalized using the expression levels of the reference gene,glyceraldehyde phosphate dehydrogenase (*GAPDH*). Asterisks indicate statistically significant differences between the overexpression and WT strains according to the Students T' test (p value < 0.05).

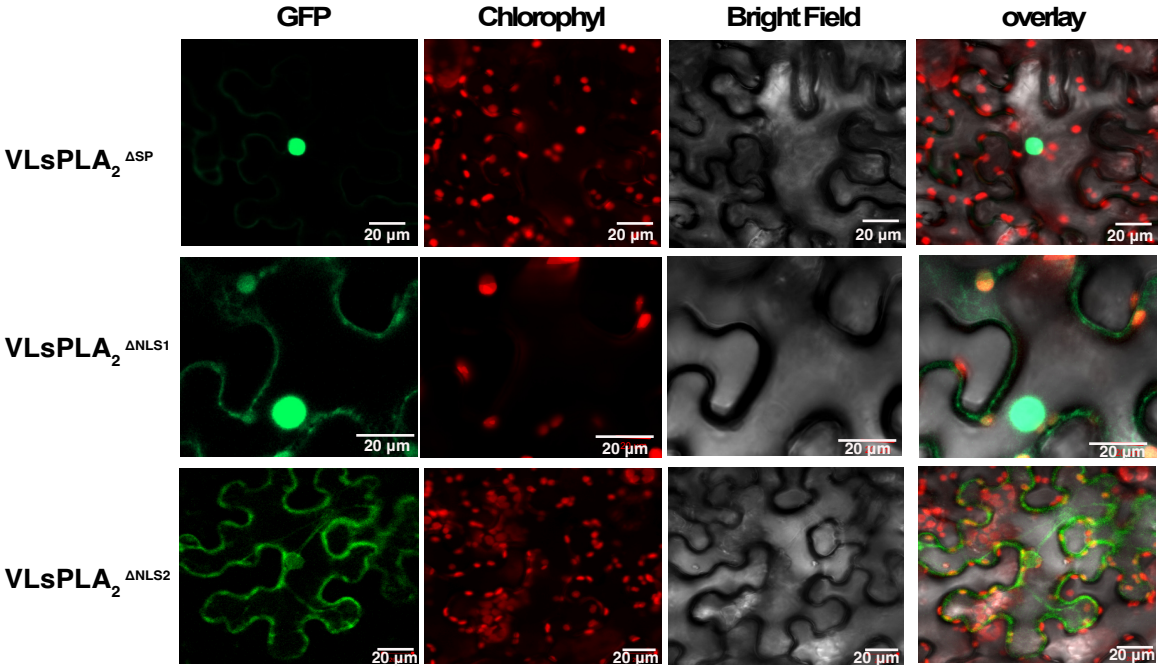

Supplementary Figure S4. Live-cell imaging of VlsPLA$_2$ mutants where signal peptide (VLsPLA$_2$ $^{\Delta SP}$), or NLS1 (VLsPLA$_2$ $^{\Delta NLS1}$), or NLS2 (VLsPLA$_2$ $^{\Delta NLS2}$) were truncated. Mutants tagged with GFP at the C-terminal and Agro-infiltrated *N. benthamiana* leaves. The localization was monitored with a laser-scanning confocal microscope with a sequential scanning mode 48 hours post infiltration. The GFP and the chlorophyll were excited at 488 nm. GFP (green) and chlorophyll (red) fluorescent signals were collected at 505– 525 and 680–700 nm, respectively.

a

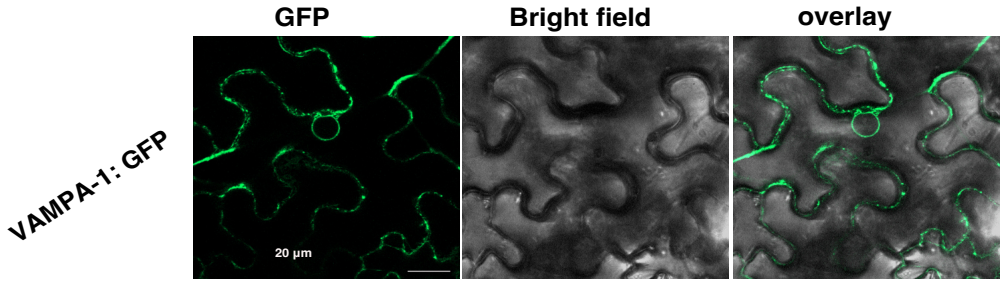

b

```
NbS00015616g0001.1      IQPWDSCFIRV-------------------------------------TLQAQKEYPLDM    73
NbS00038240g0008.1      IHPWDSCFIRVVHPNTDILLWFHLSRNMRHPFNGWFSYIVLNFVMSLVTLQAQKEYPPDM    103
NbS00060499g0005.1      IKPKSTYDFTV-------------------------------------TMQAQRTAPSDM    81
NbS00002269g0003.1      VLPRSRSNVTV-------------------------------------TMQPQTELPPDM    81
NbS00011956g0004.1      ------------------------------------------------TMQAQKEAPPDM    30
NbS00056068g0004.1      ------------------------------------------------TMQAQKEAPADM    32
NbS00026343g0007.1      VLPGSSCNVTV-------------------------------------TMQAQKEVPPDM    83
NbS00019865g0007.1      VLPGSSCNVTV-------------------------------------TMQAQKEAPPDM    83
NbS00032336g0008.1      VMPHSTCDVTV-------------------------------------TMQAQKEAPPDM    81
NbS00013560g0006.1      VLPRSTCDVIV-------------------------------------TMQAQKEAPADM    83
                                                                         *:* *   * **

NbS00015616g0001.1      QCKDKFLLQSTIVNND--IDELSPDTFNKESGRTVEESKLRVVYISPHSSPGHSED-FR-    129
NbS00038240g0008.1      QCKDKFLLQSTIVNND--SDELSPDTFNKDSGRTVEECKLRVVYISTHSSPGQFEDVFK-    160
NbS00060499g0005.1      QCKDKFLIQGTVVPFGTSEEEITPSMFNKDNRKYIEECKLRVVLVSPPNSPVLQPANGIS    141
NbS00002269g0003.1      QCKDKFLVQSVITNPGSTPKDINPDMFNKSGGNHVEECKLKVVYVSPPRKPSPVPEDSE-    140
NbS00011956g0004.1      QCKDKFLLQSVVASPGTTPKDITPEMFNKESGNHVDECKLRVAYVPPQ-PPSPVREGSE-    88
NbS00056068g0004.1      QCKDKFLLQSVVASSGTTAKDITPEMFNKEEGNHVEDCKLRVVYVPPQQPPSPVQEGSE-    91
NbS00026343g0007.1      QCKDKFLIQSVIAPSGTSNKDITTEMFNKEDGKVIDEFKLRVVYVP-ANPPSPVPEGSE-    141
NbS00019865g0007.1      QCKDKFLIQSVIAPSGTSNKDITTEMFNREDGKVIDEFKLRVVYVP-ANPPSPVPEGSE-    141
NbS00032336g0008.1      QCKDKFLLQSVVAGPGTTPKDITPEMFNKESGNHVDECKLRVAYVP-PQPPSPVREGSE-    139
NbS00013560g0006.1      QCKDKFLLQSVVATAGTSPKDITQEMFNKEPGRVVEECKLKVIYLPPPQPPSPVAEGSE-    142
                        *******:*..:.  .   .::. . **:.  . ::: **:*  :     *

NbS00015616g0001.1      -QSSDFTSN---------------------------------------------------    137
NbS00038240g0008.1      -QNSDVNSS---------------------------------------------------    168
NbS00060499g0005.1      KQGAPIETSMQQEKFPSGVENLPPAQTVGKNNKDIKFEEEIEVLDLGLSFAKNTESNTDE    201
NbS00002269g0003.1      -EWTSAGAS-------------------E----------------------TDLQEHG---    156
NbS00011956g0004.1      -EGSSPRAS-------------------I----------------------SENG------    101
NbS00056068g0004.1      -EGSSPRAS-------------------V----------------------SENGTVNT--    108
NbS00026343g0007.1      -EGGSPRAS-------------------L----------------------TEDESKSS--    158
NbS00019865g0007.1      -EGGSPRAS-------------------L----------------------TEDESKSS--    158
NbS00032336g0008.1      -EGSSPRAS-------------------I----------------------SENGAEFH--    156
NbS00013560g0006.1      -EGSSPGQS-------------------L----------------------TENDSQNG--    159
                         .
```

c

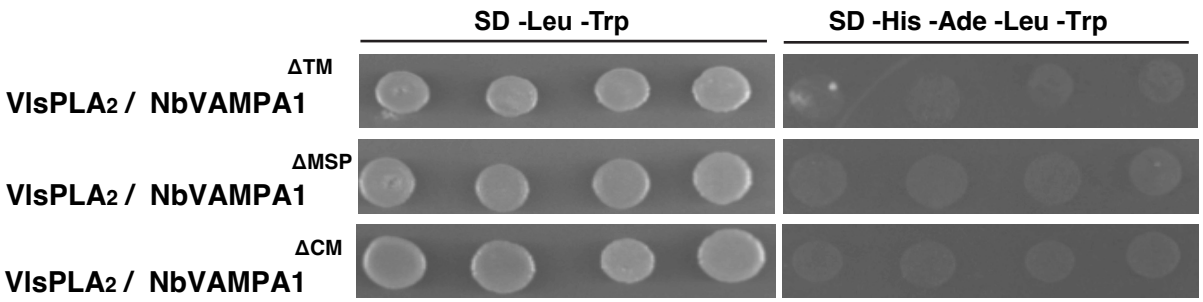

Supplementary Fig. S5. Analysis of NbVAMPA1 protein. a. Live-cell imaging of NbVAMPA-1 tagged with GFP at the N-terminal and Agro-infiltrated *N. benthamiana* leaves. The localization was monitored with a laser-scanning confocal microscope with a sequential scanning mode 48 hours post infiltration. The GFP was excited at 488 nm and collected at 505– 525 nm. **b.** Alignment of homologs to NbVAMPA1 in *N. benthamiana.* Identical sequences are marked with asterisks (*). **c.** Pairwise yeast-two-hybrid assays between $VlsPLA_2$ (used as a bait in pGBKT7 vector) and NbVAMPA1 mutated versions (used as a prey in pGADT7 vector). Growth of yeast cells on SD-4 (-His, -Ade, -Leu, -Trp) selective media represents protein–protein interaction and growth on SD-2 (-Leu, -Trp) media confirms yeast transformation